Condensation, excitation, pairing, and superfluid density in high-T_c superconductors: magnetic resonance mode as a roton analogue and a possible spin-mediated pairing

Y.J. Uemura
Physics Department, Columbia University, 538 West, 120th Street, New York, NY 10027, USA
(Dated: February 6, 2008)

To find out a primary determing factor of T_c and a pairing mechanism in high-T_c cuprates, we combine the muon spin relaxation results on n_s/m^* (superconducting carrier density / effective mass), accumulated over the last 15 years, with the results from neutron and Raman scattering, STM, specific heat, Nernst effect and ARPES measurements. We identify the neutron magnetic resonance mode as an analogue of roton minimum in the superfluid ^{4}He, and argue that n_s/m^* and the resonance mode energy $\hbar\omega_{res}$ play a primary role in determining T_c in the underdoped region. We propose a picture that roton-like excitations in the cuprates appear as a coupled mode, which has the resonance mode for spin and charge responses at different momentum transfers but the same energy transfers, as detected respectively, by the neutron S=1 mode and the Raman S=0 A1$_g$ mode. We shall call this as the "hybrid spin/charge roton". After discussing the role of dimensionality in condensation, we propose a generic phase diagram of the cuprates with spatial phase separation in the overdoped region as a special case of the BE-BCS crossover conjecture where the superconducting coupling is lost rapidly in the overdoped region. Using a microscopic model of charge motion resonating with antiferomagnetic spin fluctuations, we propose a possibility that the hybrid spin/charge roton and higher-energy spin fluctuations mediate the superconducting pairing. In this model, the resonance modes can be viewed as a meson-analogue and the "dome" shape of the phase diagram can be understood as a natural consequence of departure from the competing Mott insulator ground state via carrier doping.

PACS numbers: 74.20.Mn, 74.62.-c, 74.72.-h, 76.75.+i

I. INTRODUCTION

Since the discovery of high-T_c superconductors (HTSC), muon spin relaxation (μSR) measurements [1-3] have been applied to study magnetic order, superconducting penetration depth, and flux vortex aspects of the cuprates and other exotic superconductors. Among them, we have put a particular focus on the absolute values of the magnetic field penetration depth λ, which represents the superconducting carrier density n_s divided by the effective mass m^* as $\lambda^{-2} \propto n_s/m^*$. We discovered strong and universal correlations between the critical temperature T_c and $n_s/m^*(T \rightarrow 0)$ in various HTSC systems [4], and initiated an energy-scale argument by converting n_s/m^* into an effective Fermi temperature T_F of the superconducting carriers [5]. By combining the universal correlations and the pseudo-gap behavior, we proposed a picture for the cuprates based on crossover from Bose-Einstein (BE) to BCS condensation in 1994 [6,7]. We also demonstrated that the correlations between T_c and n_s/m^* are robust against various artificial/spontaneous formations of spatial heterogeneity, such as Cu/Zn substitution, for which we proposed the "Swiss Cheese Model" in 1996 [8].

During recent years after 1997, several important experimental results on the cuprates, relevant to the above mentioned results/pictures, have been obtained by using other techniques. They include: 1) scanning tunnelling microscope results which confirmed the "swiss-cheese" like situation in Zn doped cuprates [9], and further established spontaneous formation of spatial heterogeneity in the superconducting state in a wide range of doping levels even without impurity substitution [10,11]; 2) high-frequency conductivity measurements of n_s/m^*, which showed a frequency-dependent "dynamic" response remaining above T_c and provided the first direct evidence for a wide range of superconducting phase fluctuations in the normal state [12]; 3) the Nernst effect measurements which obtained further evidence for the dynamic superconducting response above T_c, and mapped out the region of this response as a function of external field H, temperature T, and the doping concentration x [13,14]; 4) neutron scattering studies which established that the "41 meV magnetic resonance mode", first found in YBCO [15], is generic to many of the cuprate systems, and that the mode energy accurately scales with T_c [16-18]; 5) Raman scattering studies which obtained the response in the A1$_g$ mode at $T \rightarrow 0$ whose energy precisely follows that of the neutron resonance peak [19-22]; and 6) a sharp "coherence peak" which appears in the antinodal response of ARPES studies, with the intensity proportional to the superfluid density [23].

In this paper, we wish to demonstrate that the combination of the μSR results with these new results 1) - 6) can clarify the primary determining factor for the critical temperature T_c in the cuprates and can elucidate details of their superconducting condensation and pairing mechanisms. This discussion will proceed in comparison with known cases of quantum superfluid transitions in bulk and thin films of liquid ^{4}He. In particular, we will propose a picture that the 41 meV resonance mode in the cuprates plays a role analogous to rotons in liquid He, as the key elementary excitation mode which determines

T_c. We further propose a picture of a "hybrid spin/charge roton" in an effort to reconcile apparently conflicting selection rules for the neutron magnetic resonance mode and Raman $A1_g$ mode, which are observed with the same energy transfers [19].

Consideration of dimensionality effects will lead to a new and simple account for the onset temperature of the Nernst effect and conditions necessary for dynamic superconductivity. We will compare evidence for phase separation in the overdoped cuprates, and argue that the condensation in the cuprates can be viewed as a special case of BE-BCS crossover where the pairing interaction vanishes in a moderately overdoped region. Finally, we consider a microscopic model where the motion of a charge is assisted by spin fluctuations having the *same resonating frequency*. Developing this notion, we propose a picture that the "hybrid spin/charge roton" and higher-energy antiferromagnetic (AF) spin fluctuations can be the pair-mediating bosons. These concepts naturally lead to a view in which we ascribe the anomalies in the overdoped region to the rapid disappearence of spin fluctuations due to increasing distance from the Mott AF insulator state.

II. PLOTS OF T_c VS. n_s/m^* AND T_c VS. T_F

In the vortex state of type-II superconductors, the applied field H enters into the system by forming a lattice of flux vortices, with a typical distance between the adjacent vortices $\sim 1,000$ Å for $H \sim 1$ kG. The vortex lattice and supercurrent create inhomogeneity ΔH in the internal magnetic fields, whose decay from the vortex core position is related to the London penetration depth λ. In μSR measurements, a time histogram is composed of the precession of 10^6 - 10^7 muons stopped at locations of different internal fields. In measurements with ceramic specimens, the damping of the precession envelope is often approximated by a Gaussian function $\exp(-\sigma^2 t^2/2)$, which defines the muon spin relaxation rate $\sigma \propto \Delta H$. With the London equation, one finds

$$\sigma \propto \lambda^{-2} = [4\pi n_s e^2/m^* c^2][1/(1+\xi/l)],$$

where ξ is the coherence length and l denotes the mean free path. In systems in the "clean limit" with $\xi << l$, such as the cuprates, σ represents n_s/m^*.

Figure 1 shows the accumulation of our results over the last 15 years in a plot of T_c versus $\sigma(T \rightarrow 0) \propto n_s/m^*$ in various cuprate systems [4,5,8,24-27]. These data are consistent with results from other groups [28-31]. We see that T_c increases with increasing carrier doping, following a nearly linear relationship with n_s/m^* in the underdoped region: the results from different series of cuprates share a common slope in this initial increase of T_c. Systems in the optimally doped region deviate from this linear line, showing a "plateau" like behavior, which was later found out to be due to the effect of the CuO chains in the case of the YBCO systems [29]. We see that the nearly linear trend is followed also by systems with Cu/Zn substitution [8], spontaneous formation of static magnetic regions (shown with the "stripe" symbols), and even with overdoping (Tl2201) [24], the implications of which will be discussed in later sections.

Strong correlations between T_c and n_s/m^* would not be expected from BCS theory [32], but readily expected in BE condensation. Thus, this figure gives the first strong message about possible non-BCS character of condensation in the cuprates. In fact, when one assumes m^* of the cuprates to be 3-4 times the bare electron mass, the carrier density n_s for systems in the linear region corresponds to the situation where several pairs are overlapping within an area of $\pi\xi^2$ on the CuO_2 planes, which interpolates between non-overlapping pairs in the BE limit and thousands of pairs per $\pi\xi^2$ in the BCS limit [33]. Although most of the points in Fig. 1 are obtained with un-oriented ceramic specimens, the results predominantly reflect the in-plane penetration depth and the in-plane mass, as generally demonstrated for highly anisotropic superconductors [34] with ~ 40 % correction factor between the relaxation rates from un-oriented and oriented (or single crystal) specimens.

The parameter n_s/m^* in eq. 1 represents a spectral weight of 3-dimensional screening supercurrent which causes a partial rejection of the applied field. By knowing the average interlayer distance c_{int} between the CuO_2 planes, one can obtain the 2-d area density n_{s2d} of superconducting carriers, which can be directly converted into the effective Fermi temperature $T_F \propto n_{s2d}/m^* = n_s/m^* \times c_{int}$. For 3-d systems, the results of $\sigma \propto n_s/m^*$ has to be combined with those of the Pauli susceptibility or Sommerfeld constant $\gamma \propto n^{1/3} m^*$ in the derivation of $T_F \propto n_s^{2/3}/m^*$. After this processing, we produced a plot of T_c versus T_F first in 1991 [5]. Figure 2 shows the up-to-date version of this plot, including subsequent data from varous different superconductors [33,35-39]

The T_B line represents the BE condensation temperature of an ideal Bose gas of boson mass $2m^*$ and density $n_s/2$. Although the actual superconducting T_c of the cuprates are reduced by a factor 4-5 from T_B, the trend of the underdoped cuprates is parallel to the T_B line, suggesting that the linear trend can be deeply related to BE condensation. There seems to be an empirical upper limit of T_c/T_F shared not only by the cuprates but also by other strongly correlated systems, such as organic 2-d BEDT [37], Na_xCoO_2 [39], and A_3C_{60} [35,36] systems. Figure 2 serves for classifying different superconductors between the limits of BE condensation with strong coupling (approaching towards the T_B line) and BCS condensation with much smaller values of T_c/T_F.

In Fig. 2, we also include a point for superfluid bulk ^{4}He with $T_c = 2.2$ K (blue star). Even for such a system regarded as a prototype for BE condensation, we see a 30 % reduction from its ideal-gas value of $T_{BE} = 3.2$ K, presumably caused by the finite size and interactions of He atoms. In addition to these factors, 2-dimensional aspects of the cuprates could also cause a further re-

duction of T_c from T_B as discussed in Section V. Recently, condensation of fermionic ultracold ^{40}K gas has been achieved in the BE-BCS crossover region [40]. We also plot a point for ^{40}K (red star) by multiplying 10^8 to both T_c and T_F. Interestingly, the crossover region seems to exist rather close to the T_B line for the case of ultra-cold fermion atoms in which we expect a much smaller effect of correlations compared to the cuprates.

III. BE-BCS CROSSOVER CONJECTURE

A connection between BE and BCS condensation has been a subject of theoretical interest for many decades. There exist a few different energy scales for superconductivity: a) the energy of condensing carriers represented by T_F, related to the number density and mass; b) the net attractive interaction, related to the gap energy scale in the BCS side, and to the binding energy in local bosons, and c) the energy of "pair mediating bosons" such as the Debye frequency in the phonon-coupling. The fourth energy scale d), the condensation temperature T_c is determined by the interplay among a), b), and c). Many theoretical discussions have been given, by fixing the carrier concentration (a), and artificially changing the attractive coupling (b). As a typical example, Fig. 3(a) shows the results obtained by Nozières and Schmitt-Rink [41] in 1985. Note that the horizontal axis is given for the coupling strength V, normalized to the "critical strength" V_c related to the particle density and the range of the interaction. We see that $T_c \sim T_B$ in the strong coupling limit ($1/V < 1$), while $T_c \propto V$ on the BCS side ($1/V >> 1$).

In cuprate systems, we change the carrier density (a), while the attractive energy scale (b) is not necessarily fixed. On the other hand the "mediating boson" would not change for different carrier densities. So, it would make sense to consider the case by fixing (c) and varying (a), and consider how (b) and (d) would evolve. By combining the results in Figs. 1 and 2 with the pseudogap behavior which was then-noticed in NMR (spin gap) [42,43] and c-axis conductivity [44] (insulating below T^*) studies, we proposed a picture shown in Fig. 3(b) in 1994 [6,7] to map the situation of the cuprates to BE-BCS crossover. We argued that the underdoped region corresponds to the BE side, where the pair formation temperature T_{pair} maps to T^* below which one expects gradual formation of the spin singlet pairs. On the BCS side T_{pair} and T_c should be very close, since the condensation occurs immediately after the pair formation. These two regions may be separated by whether the interaction is non-retarded (BE side) or retarded (BCS) side.

Independent from our picture, Emery and Kivelson [45] presented the phase-fluctuation picture shown in Fig. 3(c) in 1995, and interpreted the μSR results as a signature for a Kosterlitz-Thouless (KT) type transition [46] expected in 2-dimensional systems where superconductivity is destroyed by thermal excitations of phase fluctuations. Although their picture in Fig. 3(c) shares various fundamental spirits with the BE-BCS crossover pictures, some important differences exist as discussed in later sections. The overdoped region of the cuprates, which corresponds to the "BCS" side of Figs. 3(b) or 3(c), turns out to be quite different from the simple BCS systems as discussed in Section VIII. Various types of models based on BE condensation [47,48] and BE-BCS crossover [49] have also been proposed to account for HTSC.

IV. HETEROGENEITY

The relevance of BE condensation also appears in the robustness of the cuprates against heterogenous spatial media. The first signature of this came in our study of Zn-doped YBCO and LSCO systems in 1996 [8]. As shown in Fig. 4(a), the reduction of n_s/m^*, as a function of Zn concentration, can be explained very well if we assume that Zn creates a non-superconducting region around it in an area of $\pi\xi^2$ on the CuO_2 planes. The solid line in Fig. 4(a), representing this "swiss cheese model" agrees well with the data *without any fitting*. A few years later, this situation was directly confirmed by the scanning tunnelling microscope (STM) studies [9], as shown in Fig. 4(b).

In Eu doped $(La,Eu,Sr)_2CuO_4$ (LESCO), regions with static incommensurate magnetic order is formed spontaneously even in superconducting specimens [26]. The volume fraction of regions with static magnetic order shows a one-to-one trade off with the total value of n_s/m^*, as shown in Fig. 4(c), indicating that the "magnetic island" regions do not support superfluid. Thus the situation looks again like the "swiss cheese", with "non-superconducting magnetic islands" replacing the "normal area around Zn". In zero-field μSR measurements of oxygen overdoped $La_2CuO_{4.11}$ [25], we found the average size of such magnetic islands to be comparable to the in-plane coherence length $\xi \sim$ 15-30 Å in radius. The Zn-doped and magnetic-island systems follow the same trend as other less perturbed underdoped cuprates in Fig. 1.

Recently, spontaneous formation of spatially heterogeneous areas, with similar length scales, was discovered by a series of STM measurements [10,11] in under to optimally doped Bi2212 systems without impurity doping. As shown in Fig. 4(d), the STM "gap map" clearly demonstrates a decomposition of the system into regions with a sharp superconducing gap (orange to red colors) and a broad pseudo-gap like response (blue to black colors). Upon doping carriers, the former region increases in volume fraction, which roughly follows the behavior of n_s/m^* [50]. The new STM results suggest a possibility that the underdoped cuprates are analogous to "spontaneously formed swiss cheese". We shall see later that overdoped Tl2201 also exhibits yet another type of spatial heterogeneity / phase separation.

Thus the nearly linear trend in Fig. 1 for all these systems represents a generic feature of the cuprate superfluid, which is impressively robust against the formation

of spatial heterogeneity. This is a feature which we can expect for a superfluid of tightly bound bosons, as we shall see in the next section, but not for BCS systems where impurities can scatter an individual carrier before it appreciates an attractive interaction with its pair in a retarded process.

V. TWO DIMENSIONAL ASPECTS

Let us now compare the cuprates with the superfluid transitions in thin films of ^{4}He and ^{4}He/^{3}He mixtures in regular and porous media. Figure 5(a) shows the temperature dependence of the superfluid density of a ^{4}He film on Mylar [51] and the relaxation rate $\sigma(T)$ in oriented optimally-doped YBCO [52] (multiplied by a correction factor of 1/1.4) and (Y,Pr) substituted underdoped YBCO [27]. The superfluid density of ^{4}He film is almost independent of temperature until the KT transition suddenly drives the system into the normal state. In contrast, the superfluid density of YBCO shows a strong reduction with increasing T: the low-T variation was attributed to the excitation of nodal quasiparticles in the d-wave energy gap [53].

Figure 5(b) shows a plot of the superfluid transition temperature T_c versus the 2-d superfluid density of ^{4}He films on regular (Mylar) [51] and porous (Vycor) [54] media and ^{4}He/^{3}He mixture adsorbed on fine alumina powders [55]. The Mylar results represent the case with the smallest perturbation, comparable to the simple hole-doped cuprates. The Vycor results are analogous to the Zn-doped cuprates: normal regions are formed around the pore wall or around Zn impurities in order to help smooth flow of the superfluid. The ^{4}He/^{3}He mixture corresponds to the overdoped cuprates as discussed later. Yet with different degrees of perturbation, T_c precisely follows the linear relationship predicted by the Kosterlitz-Thouless theory [46]. The robustness against heterogeneity is common to the case of the cuprates in Fig. 1.

By multiplying the interlayer distance c_{int} with n_s/m^*, we can produce a corresponding plot for the cuprates with the horizontal axis representing 2-d area superfluid density n_{s2d}/m^*, as shown in Fig. 5(c) [56]. We find that: (1) the systems with different c_{int} exhibit distinctly different slopes; (2) the $T \rightarrow 0$ values of n_{s2d}/m^* is more than a factor of 2 larger than the "KT-jump" value $n_{s2d}/m^*(T = T_{KT})$ expected by the KT theory shown by the T_{KT} line [57]; and (3) $T_c \propto 1/c_{int}$ from the early studies of YBCO/PrBCO sandwich layer systems [58]. These features indicate that the simplest version of the KT theory for 2-dimensional systems is not adequate to account for the transition temperatures of cuprtates. This point was missing in the argument of Emery and Kivelson [45].

For a non-interacting Bose gas with a parabollic energy dispersion, BE condensation does not occur in purely 2-dimension. However, one can expect condensation via inclusion of a small 3-d coupling [47,48] and/or dispersion with the power to k lower than 2 [59]. A small 3-d coupling for a quasi 2-d Bose gas would provide a logarithmic dependence of T_c on the coupling strength [47,48], which decays exponentially with interlayer distance in the WKB approximation for the interlayer tunneling. This would lead to the relation $T_c \propto n_{s2d}/m^* \times 1/c_{int} = n_s/m^*$ [56] which explains the trends in Figs. 1 and 5(c).

As illustrated in Fig. 5(c) with the blue arrow, the superfluid density of the cuprates is substantially reduced from the $T \rightarrow 0$ value before reaching the T_{KT} line, where the thermal creation of vortex/antivortex pairs could destroy the superconducting state if there is no interlayer coupling. For a substantial 3-d coupling, the vortex pair creation is further suppressed, and $n_s/m^*(T)$ can be further reduced. Thus a key to understanding the correlations in Figs. 1 and 5(c) would be to identify the process which governs the thermal reduction of n_s/m^*.

VI. EXCITATION: MAGNETIC RESONANCE MODE AS A ROTON ANALOGUE

In bulk 3-d superfluid ^{4}He, the transition temeprature $T_c = 2.2$ K is determined by the phonon-roton dispersion relation shown in Fig. 6(a) [60]. The system loses superfluidity with this mechanism well below $T_{BE} = 3.2$ K. Although its energy $\hbar\omega_{rtn}$ corresponds to about $4k_BT_c$, the thermal excitation to the roton minimun has a large weight in the phase space thanks to a substantial momentum transfer of $\sim 2.0\mathring{A}^{-1}$, and $\hbar\omega_{rtn}$ becomes a primary determining factor for T_c. This situation can be appreciated by looking at the linear relation between the $\hbar\omega_{rtn}$ and T_c in bulk ^{4}He at different pressures [61], shown in Fig. 6(b), although only a small change is measurable.

It is then natural to search for any counterpart of rotons in the cuprates. Here we propose the (π,π) S=1 magnetic resonance mode, observed by neutrons, as excitations playing a role analogous to that of rotons. In Fig. 6(b), we plot T_c versus the energy of this mode $\hbar\omega_{res}$, determined by neutron scattering for various cuprate systems [15-18]. We also include the peak energy $\hbar\omega_{A1g}$ of the A1$_g$ mode observed in Raman scattering [19-22], which closely follows the resonance mode energy. We see an impressive linear dependence of T_c on $\hbar\omega_{res}$ and $\hbar\omega_{A1g}$ for wide variety of cuprates. The slopes of the linear relationships for cuprate-resonances and He-rotons are different only by 20 % or so.

At a glance, the magnetic resonance mode is quite different from rotons, since it does not create a liberated spin-singlet charge pair nor charge density modulation, except through a mechanism which we will propose in the next section. However, the following argument may enlighten further similarities between these excitations. The roton minimum represents a soft phonon mode towards solidification of He, which has not yet been achieved, at the momentum transfer close to that of the "Bragg point of the solid He to-be". So, it can be viewed as an excitation mode directly related to the "yet-to-be-stabilized ground state" competing with the superfluid

ground state.

For underdoped cuprates, likely ground states competing against the superconducting state include the antiferromagnetic (AF) state and the stabilized incommensurate/stripe spin state. Since the AF state developes around the momentum transfer (π,π), the S=1 magnetic resonance mode can be viewed as an excitation related to this "yet-to-be achieved and competing ground state". The stripe state develops around an incommensurate wave vector. Recently, the downward dispersion of the resonance mode towards this incommensurate wave vector was noticed by neutron studies [15,62]. So, the incommensurate/stripe state could also be viewed as a competing ground state connected to the resonance mode. Indeed, in $La_2CuO_{4.11}$, the magnetic islands with stabilized incommensurate spin correlations coexist with surrounding superconducting and non-magnetic regions [25]. So, the superconducting and stripe states should have very close ground state energies and be competing with each other.

An important notion about rotons is that the excitation is not to create the competing ground state itself, but is to populate "excitations" assciated with that competing state. The AF state or the incommensurate spin state is the spin singlet S=0 state. So, the magnetic resonance mode represents the "S=1 excited state" of the "unachieved S=0 AF state". This is a way to understand the S=1 excitation as an acceptable candidate for the roton analogue. "Rotons as soft phonons" in ^{4}He are *excitations* associated with the unachieved solidified He lattice.

We also have to realize that the thermal excitations of the magnetic resonance mode could contribute towards reduction of the superfluid density n_s/m^*. This feature can be found in earlier "spin-exciton" theories of Norman and co-workers [63,64] as well as "topological transition" theory of Onufrieva and Pfeuty [65]. Though the relationship to the superfluid density was not explicitely discussed in both theories, the resonance mode is described as a particle-hole excitation from the superconducting ground state. Thus the excitation of the resonance mode should reduce n_s/m^*. In other words, the superconducting ground state can be destroyed via excitations associated with the (yet-to-be-achieved) spin ordered state in the same way as those associated with charge ordered states. Now we can view the magnetic resonance mode in the cuprates as the excitation analogous to rotons in superfluid He as well as "magneto-rotons" in fractional quantum Hall systems [66].

In the cuprates, the resonance mode energy is related to the "distance from the competing ground state". Thus $\hbar\omega_{res}$ increases with increasing doping as the system moves farther away from the AF ordered state. It has been difficult to observe the resonance mode by neutron scattering in the La214 systems. However, if we adopt the Raman $A1_g$ results, T_c of the 214 system also follows the linear relation with the mode energy, as shown in Fig. 6(b). The resonance mode appears more clearly in the low-energy dispersing branch at the incommensurate position in LSCO [62]. In Fig. 5(b), we include the energy at $(\pi-\delta,\pi)$ in YBCO [17] and LSCO [62], which exhibits an even better agreement with the slope of rotons.

In theoretical works for the resonance mode, we often find statements such as "the reason is unknown for why the mode energy scales with T_c". We claim here that T_c is determined by the mode energy via thermal excitations of the mode which reduce superfluid density. The actual situation can, however, be somewhat more complicated since not only the resonance mode but also the "continuum" excitations (or the $B1_g$ Raman modes) would contribute towards reduction of the superfluid density in the cuprates, and the energies of the resonance and continum modes are very close to each other.

VII. RECONCILIATION OF RAMAN AND NEUTRON MODES

Raman scattering usually probes spinless charge excitations at nearly zero net momentum transfer. How, then, can we explain the Raman $A1_g$ mode to detect the S=1 magnetic resonance mode which involves spin-flip and momentum transfer of (π,π) ? This is still a remaining open question. Possible but seemingly unlikely answers could include a spin-flip Raman mode involving spin-orbit coupling, detecting spin fluctuations near k = 0 within the "shadow AF zone" dispersion corresponding to (π,π). A standard two magnon Raman mode cannot explain the same energy transfer of the Raman and neutron peaks, since in that case the Raman $\hbar\omega_{A1g}$ should have been a factor of 2 larger than the neutron $\hbar\omega_{res}$. In superfluid ^{4}He, simultaneous creation of two rotons is known to give a strong Raman signal [67], assuring momentum conservation with nearly opposite momentum transfers of the two rotons.

Recently, STM studies [11,68,69] found evidence for inelastic charge modulations spreading with the periodicity of 4 lattice constants, which could provide yet another/relevant competing ground state. Dung-Hai Lee and co-workers [70], and some other authors [71] proposed a picture involving a roton minimum for this charge density modulation. In general, any such charge or spin excitations relevant to competing ground states could play a role similar to the resonance mode as discussed here. However, we shall note that the contribution of modes with small momentum transfers would provide a limited effect in the reduction of T_c due to its limited phase space factor. In this sense the (π,π) resonance mode is the most attractive candidate for the primary determining factor of T_c.

Struggling with the question about the almost identical energies of the S=1 neutron resonance and presumably S=0 Raman mode can bring a further possible insight into the roton-like mode in the cuprates. In $(La,Nd,Sr)_2CuO_4$, which shows stabilized stripe spin and charge modulations, neutron scattering [72] found mag-

netic incommensurate satellite Bragg peaks (red close circle in Fig. 6(c)), away from the AF zone center (π,π) by a distance δ in momentum space due to spin modulation. Also observed simultaneously are the the lattice deformation peaks at a distance 2δ away from the lattice zone center (blue closed circle in Fig. 6(c)), due to the charge modulation. Since the cuprate systems exhibit a preference of δ being $2\pi/8$, a spin/charge ordered stripe state with $\delta = 2\pi/8$ can be a natural strong candidate of the "competing ground state". Having the periodicity $2\delta = 2\pi/4$, the charge modulation observed by STM can well be a manifestation of this stripe modulation or similar 2-d incommensurate correlations in a dynamic response.

Suppose the superconducting ground state wins in the competition against this incommensurate state. This will lift the energy of both the magnetic and charge satellite Bragg peaks to finite energy transfers and create the magnetic resonance mode near the magnetic satellite as well as the charge modulation mode near the charge satellite. These spin and charge modes should co-exist simultaneously. The energy of these modes is determined by the energy difference between the superconducting state and the stripe state. Therefore, we would expect the **same energies** for the charge and spin modes, but these modes exist, of course, with different momentum transfers. This special situation creates a novel roton-like excitation in cuprates with double charge and spin minima, as illustrated in Fig. 6(c). We shall call this as a "hybrid spin/charge roton".

This double-minima hybrid roton provides a natural resolution for the neutron vs. Raman conflict. The S=1 magnetic neutron mode is due to the spin branch while the Raman results can be understood as the manifestation of the charge/lattice branch, which would show up as the S=0 response near the zone center. It is then natural to find these modes with the same energy transfer, as actually observed in experiments shown in Fig. 6(b).

Rotons are usually viewed as representing the density modulation in neutral superfluids, and charge modulation in charged superconductors. The spin mode in cuprates, however, can exist only if the dynamic combined spin-charge modulation assures that this mode is associated with the "to-be-achieved" static spin-charge modulated ground state. Therefore, the existence of the spin mode directly implies simultaneous dynamic charge modulation. This argument gives the basis for why the excitation of the magnetic resonance mode can contribute to the reduction of the superfluid density n_s/m^*, or in other words to the destruction of superconducting order parameter, in the cuprates.

In charged superfluids and/or metals, the $k = 0$ response of the density fluctuations corresponds to plasmons, which usually exist at a rather high energy transfer. Then, one tends to presume a steep reduction of the charge-roton branch towards the $2\delta = 2\pi/4$ minimum from the zone center, instead of a rather modest energy reduction shown in Fig. 6(c). The in-plane plasma frequency ω_p at $k = 0$ for the optimally doped YBCO system, determined by optical conductivity [73], has an energy scale at least one order of magnitude higher than that of the 41 meV mode energy. This energy scale is also represented roughly by T_F obtained by the superfluid density in Fig. 2, as the product of λ and ω_p is the light velocity. These energies represent "real responses of the superconducting ground state".

In the parent Mott insulator, all the charges are localized, and thus the plasma frequency is pushed down to zero, since the effective mass is infinitely large. Just as the magnetic mode energy represents the low-energy spin waves of the *yet-to-be achieved Mott insulator AF state*, the charge branch in Fig. 6(c) should be considered for a *hypothetical situation* with a charge injected into a Mott insulator, somewhat comparable to the case of photo-induced conductivity experiments of a parent insulator system. Then, one might understand the very low energy scale, which could be related predominantly to nearly localized charges. Another way to view the roton branches: suppose we temporarily created a small island region of the "un-achieved competing ground state", corresponding to a vacancy in the "swiss cheese", by supplying the finite energy transfer to the superconducting system, and study *excitations* within that island. Then we will find all the roton-like branches. This argument explains why the energy of the charge mode at the zone center $k = 0$ can be identical to that of the magnetic mode at (π,π). More formally, this spin-charge coupling would provide terms analogous to the case of strong spin orbit coupling, giving some qualification to the "seemingly unlikely" argument of spin-flip Raman scattering described in the beginning of this section. However, one has to wait for further accumulation of experimental studies to clarify details of the "charge branch" near the zone center and its interplay with the lattice and spin degrees of freedom.

VIII. PHASE SEPARATION IN THE OVERDOPED REGION

In 1993, our group [24] and a European μSR team [30] independently found a very strange variation of n_s/m^* in overdoped Tl2201. As shown in Fig. 1, n_s/m^* decreases with increasing carrier doping, yet conductivity studies imply no anomaly in m^*. We presented a picture involving phase separation into superconducting and normal metal ground states [24,7], while authors of ref. [30] interpreted this in terms of pair-breaking scattering. Co-existence of superconducting and normal charges at $T \to 0$ in Tl2201 also shows up in specific heat measurements by Loram *et al.* [74] shown in Fig. 7(a). Upon overdoping from the highest T_c sample in the nearly optimum region, the "un-gapped" response develops in the T-linear term $\gamma = C_{el}/T$ of the electronic specific heat C_{el}. As shown in Fig. 7(b), the "gapped" fraction, presumably representing the volume fraction of the superconducting region, closely follows the variation of the su-

perfluid response n_s/m^* obtained from μSR [24].

Further evidence of co-existing gapped and ungapped ground states can be found in the height ΔC of the specific heat jump at T_c. In BCS superconductors, the height ΔC at T_c is proportional to T_c, as illustrated in Fig. 7(c). In the γ versus T plot, ideal BCS systems with different T_c's should exhibit the same jump height $\Delta C/T_c$, as illustrated in Fig. 7(d). Comparison of Figs. 7(a) and 7(d) demonstrates that the superconducting condensation in overdoped Tl2201 occurs only in a finite volume fraction. Thus the overdoped system is fundamentally different from standard BCS superconductors where all the normal-state charge carriers participate in the superfluid n_s once the energy gap is developed around the entire Fermi surface. The jump height $\Delta C/T_c$ follows the trend of n_s/m^* and the gapped volume fraction, as shown in Fig. 7(b), further reinforcing this argument.

Similar behavior in the other overdoped cuprates have been found by subsequent μSR measurements in YBCO with (Y,Ca) substitution [75] and in CaLaBaCuO [31], and torque measurements of Hg1201 [76]. Other signatures of this anomaly include the un-gapped response in optical conductivity [77] in optimal to overdoped YBCO, and the recombination time of photo-induced anti-nodal quasiparticles which becomes independent of laser excitation power in the overdoped region of Bi2212 [78]. All these results indicate that the overdoped cuprate systems have a substantial number of unpaired fermion carriers in the ground state. As a condensed boson superfluid coexisting with fermionic carriers, the overdoped cuprates strongly resemble ^{4}He/^{3}He mixture films. Indeed the T_c versus n_s/m^* relationship in these two cases follow very similar behaviors, as shown in Figs. 1 and 5(b).

IX. PHASE DIAGRAMS AND THE NERNST EFFECT

A. phase diagrams

In recent years, we presented a generic phase diagram for the cuprates [79,33] shown in Fig. 8(a), which is a hybrid of the BE-BCS conjecture and the phase separation picture in the overdoped region. We assume that the pairing energy, represented by T^*, vanishes *within* the superconducting dome at a critical concentration p_c in a modestly overdoped region. Tallon and Loram [80] obtained $p_c \sim 0.19$ holes per Cu for YBCO, Bi2212 and LSCO systems, while Hwang *et al.* [81] obtained $p_c = 0.23$ for Bi2212, and some other estimate [82] suggeests that p_c could be even larger in LSCO, as illustrated in Fig. 8(b). These subtle differences may be partly due to different definitions used to derive T^* from results of various experimental methods. It is also possible that p_c substantially varies from system to system.

In our view, the phase separation in the overdoped region occurs to save condensation and pairing energies at a cost of (screened) Coulomb energy necessary for disproportionation of charge density [79]. Without taking into account the possibility of phase separation, the authors of refs. [80] and [81] argued that the existence of superconductivity at the hole concentration $x > p_c$ could rule out a positive role played by the pseudogap state for superconductivity. Our phase separation picture, however, presents a counter-example to this argument and shows that the superconducting state can exist at $x > p_c$ with T^* representing the onset of an interaction **necessary** for superconductivity.

The reduction of T^* with increasing doping is well established by many experimental results. However, this is not a feature readily expected in a general argument of BE-BCS crossover. In fact, if the pair formation energy did not show a strong dependence on doping, we could expect T_c to rise smoothly up to the T^* energy scale with increasing doping, after which the system slowly crosses over to a standard BCS behavior with all the normal state carriers condensing in the superconducting state without spatial phase separation. T_c would still come down gradually in the high-density limit due to the effect of retardation. Compared to this "standard BE-BCS crossover", the situation in the cuprates is different, because the "origin of pairing interactions" seems to die away as the doping progresses.

B. Nernst effect

The results of the high-frequency superconducting response [12] and the Nernst effect [13,14] demonstrate the existence of vortex fluctuations (or "superconducting phase fluctuations" or "dynamic superconductivity") in a wide region of the normal state above T_c, as shown in Fig. 8(b) [83]. In thin films of ^{4}He, the corresponding region exists above the superfluid temperature $T_c = T_{KT}$ up to the "mean-field" superfluid energy scale whose upper limit can be given by the lambda transition temperature 2.2 K of the bulk ^{4}He. This comparison leads us to realize that the "Nernst region" could have been superconducting if the system were protected against various origins for the destruction of the superconducting states, including low dimensional aspects, excitation of roton-like modes, etc., but all the other necessary characters for superconductivity were conserved. Then, the onset temperature T_{on} of the Nernst effect corresponds to T_c of such a "hypothetical 3-d and roton-less counterpart" of highly 2-d cuprate systems.

In Fig. 2, we include a point (green star) having T_F of $La_{1.9}Sr_{0.1}CuO_4$ in the horizontal and the Nernst onset T_{on} of the same system [13,14] on the vertical axes, respectively. Interestingly, this point for "hypothetical underdoped LSCO" lies very close to the T_{BE} line, similar to those of bulk ^{4}He and ultracold ^{40}K. This suggests that the effect of pair overlapping in the very underdoped region may be modest, and/or the coherence length could be comparable to the intercarrier distance. Indeed, the new estimate for ξ from the Nernst study [14] supports

the latter picture.

For further doping, T_{on} is suppressed because T^* is reduced. It is important, however, to realize that the pair formation energy scale T^* and the on-set of dynamic superconductivity T_{on} represent two distinctly different energy scales on the BE side. Pair formation can occur at any high temprature if a strong attractive force is provided, while the fluctuating superconductivity is possible only below T_{BE}. Observation of the Nernst effect above T_c does not distinguish between BE and BCS type condensations, since a thin film of a typical BCS superconductor can also exhibit the Nernst effect above T_c. The more important feature for underdoped cuprates is the large region in the T-x phase diagram above T_{on} but below T^*, as shown in Figs. 8(a) and (b), where one would expect the emergence of normal but paired (2e) charge carriers coexisting with unpaired (e) carriers.

The observation of Nernst effect above T_c does not necessarily imply KT like phase-fluctuations as the primary determining factor for T_c. In low-dimensional magnetic systems, we expect correlated spin fluctuations in a large temperature region above the 3-d ordering temperature, for both cases with or without a KT transition. Analogous to this, one can expect the Nernst effect for any superconducting system with strong anisotropy, where T_c is reduced from the 3-d values but the transition temperature is still governed by the anisotropic coupling strength. Furthermore, excitations of roton-like modes would create liberated vortices and thus also contribute towards the Nernst signal.

C. determining factor for T_c

In Fig. 1, the trajectory for the La214 systems exhibits "early departure" from the linear line of YBCO and other cuprates. La214 systems have a particular closeness to competing magnetic ground states as demonstrated by the instability against spin/charge stripe formation near the 1/8 concentration. Then, we can ascribe the reduced T_c (about a factor 2 smaller than that of YBCO for a given n_s/m^*) to the reduced (and likely broadened) resonance mode energy.

In bulk superfluid ^{4}He, T_c is related to the particle density, mass, and the roton energy. The roton energy provides a proper account for the reduction of T_c from T_{BE} due to the finite-boson-size and interaction effects. In thin-films of He, T_c is determined primarily by the particle density and mass via the KT transition, since the roton energy there would be much higher than T_{KT}. In underdoped cuprates, as we have seen, T_c seems to be related to the doped hole density and mass as well as to the resonance mode energy. The mode energy will become higher with hole doping as the system becomes distant from the AF state, while the increasing superfluid density would also help lowering the energy of superconducting state. Both of these would help increasing T_c approximately linearly with the doping x.

However, the decrease of T^* with increasing x implies that the origin of superconducting pairing is destroyed gradually with increasing hole density x. In other words, the distance from the competing AF Mott insulator state helps increase the roton-like resonance energy while decreasing the coupling strength of superconducting pairs. This situation can be expected if the AF interaction provides the very origin of pairing.

X. A MICROSCOPIC MODEL FOR PAIRING MEDIATED BY SPIN FLUCTUATIONS

A. motion of a charge resonating with AF spin fluctuations

Stimulated by this possibility, we now develop a microscopic model for a unique motion of a charge in nearly AF but actually metallic cuprate systems. Let us consider how a charge (hole) motion can avoid creating frustration in the region with a short-range and dynamic AF correlations. We start with a story for a single hole illustrated in Fig. 9(a). The surrounding AF configuration is fluctuating with the frequency ω_{AF}, which implies that all the surronding Cu spins change their directions within half a period π/ω_{AF}. If the charge hops to the adjacent site at this half period, then there is no extra spin frustration in the surroundings, see Fig. 9(b). During the next half period of spin fluctuations, the charge could further hop to the next adjacent site, as Fig. 9(c). If the charge motion occurs this way, sequenced with the spin fluctuation, extra spin frustration can be avoided. Charge motion of any other (higher) frequency would make a mis-match with the spin lattice, and thus cost extra energy for creating frustrated magnetic bonds.

For a charge proceeding towards the Cu-O-Cu bond direction [i.e., the (π,0) direction in the reciprocal space], this implies that within the full period of spin fluctuations, the charge proceeds by 2 lattice constants. This charge motion has the wavevector $2\pi/2a$, corresponding to that of the "antinodal charge" at the (π,0) point of the Brillouin zone. So, the antinodal charge can proceed comfortably in the nearly AF environment, if its frequency (kinetic energy) "resonates" with the frequency of the AF spin fluctuations. A specially strong spin-charge coupling can be expected for the case with $\hbar\omega_{antinode} = \hbar\omega_{AF}$.

This situation can be viewed as a charge motion creating the AF fluctuation with the frequency $\hbar\omega_{AF} = k_B T_F$, just as a motion of a charge in BCS superconductors creates a phonon. Analogous to BCS coupling mediated by a phonon, the AF fluctuating environment created by the first charge motion in the cuprates can be appreciated by the arrival of the second charge. This would support coupled charges with a strong attractive interaction mediated by spin fluctuations.

In reciprocal space, this implies connecting the antinodal charges with AF fluctuation as illustrated in Fig.

10(a). An initial charge at $(0,-\pi)$ creates a (π,π) AF fluctuation and ends up in $(\pi,0)$ charge in the final state. The same AF fluctuation can be absorbed by another charge having initial state of $(0,\pi)$ which is scattered into $(-\pi,0)$. The large energy gap in the antinodal positions, opening below T^*, would be a manifestation of the strong coupling of antinodal charges via this mechanism. In this case the spin fluctuations are analogous to phonons in BCS coupling as a "virtual" boson in the "scattering" process. However, the direct coupling between the $(\pi,0)$ and $(-\pi,0)$ charges is not supported since the AF (π,π) wavevector does not connect antinodal charges with opposite momentum directions.

B. coupled nodal charges and the resonance mode as a pi-meson analogue

Let us now consider the motion of a single nodal charge at $(\pi/2,\pi/2)$ in the Brillouin zone. To achieve propagation along the nodal direction, this charge should hop, after the first hop in Fig. 9(b), towards the perpendicular direction from the first hop, leading to the state shown in Fig. 9(d) after one period of the AF spin fluctuation. In this case, the charge has moved the distance corresponding to the diagonal of the unit CuO_2 square lattice, inferring the corresponding wavevector (π,π), twice as large as that of the nodal carriers. Due to this complete mismatch, the single nodal carrier cannot appreciate benefit of the "resonating motion". However, the (π,π) AF fluctuation can connect two nodal charges, with opposite momentum directions, as shown in Fig. 10(b). This process provides a stable "bound state" of two nodal charges, with the AF spin fluctuation playing a role of the Yukawa meson in the binding of hadrons in nuclei.

The energy of the AF fluctuation mediating this direct coupling is related to the size of the boson, similarly to the pion mass related to the size of deuteron nucleus, and also similarly to the energy gap related to the coherence length in BCS superconductors. We note that the resonance mode energy of ~ 41 meV is just appropriate for creating a boson having the size of coherence length $\sim 10-20$ Å in the cuprates. Thus we suggest the possibility that the magnetic resonance mode can be the pair mediating boson for nodal charges.

C. nodal vs. antinodal carriers and ARPES coherence peak

As discussed in earlier sections, we also expect the existence of "the charge branch" of the hybrid spin/charge roton, and/or higher energy charge fluctuations, which could cause scattering of nodal charges with a rather small momentum change within the "nodal hole pocket", as shown in Fig. 10(d), to contribute to an additional scattering process for an attaractive interaction. Nearly AF spin fluctuations can also contribute to this type of scattering process between the two different nodal hole pockets across the zone center, in addition to the direct binding.

When the charge branch excitation couples two antinodal particles near the $(0,-\pi)$ points, one of them can be viewed as a $(0,+\pi)$ particle in an Umklapp process, as illustrated in Fig. 10(c). Then the charge branch roton can be the direct "binding boson" of antinodal charges, similarly to the spin branch for nodal charges. Since the ARPES measurements probe spin-non-flip S=0 charge processes, and since the coherence peak selectively appears in antinodal responses, the ARPES coherence peak can be viewed as the process of detecting/liberating the charge-branch roton via energy supplied by a photon, analogous to the Raman $A1_g$ mode. Figures 10(e) and (f) compare this process with neutrons creating the magnetic resonance mode for nodal particles. In these "liberation processes" of binding bosons, we expect the intensity to be proportional to the number of condensed bosons. This is similar to pion creation with accelerated particle beam, in which the intensity is proportional to the number of nucleons existing in the production target. This argument explains why the ARPES coherence peak and neutron resonance peak both appear with intensities proportional to the superfluid density n_s/m^*.

The interplay between the "scattering" process (Fig. 10 (a) and (d)) and the "binding" process (Fig. 10 (b) and (c)) is reminiscent of the Feshbach resonance [40,84] appearing in the BE-BCS crossover of ultracold atoms. Note that some of these processes in Fig. 10, such as the binding ones in (b) and (c), may take place simultaneously / cooperatively as combined spin/charge fluctuations, as discussed earlier. In the Hamiltonian of such coupled processes, the spin fluctuation operator (green line in Fig. 10) and the charge fluctuation operator (light blue line) might appear together, operating simultaneously on the wave function composed of a combination of the nodal and antinodal wavefunctions. This strong spin-charge coupling may not be confined to the case of the low-energy hybrid roton in (b) and (c), but could also exist in scattering processes with higher energy fluctuations shown in (a) and (d). Then we expect high energy charge fluctuations to appear with the same energy transfers as that of the high energy AF spin fluctuations spreading over the energy region up to about 100-200 meV or so. The inelastic charge modulation recently observed by STM appears exactly in this energy region with the momentum transfer close to that of the charge branch of the hybrid roton. Thus, this STM signature can be viewed as a manifestation of the counterpart of the AF spin fluctuations. Other possible signatures of the corresponding dynamic charge modulations include the line profile of ARPES antinodal intensities near 100 - 150 meV, and the "mid-infrared reflection" observed in optical conductivity measurements in this energy region.

Being originally an antiferromagnetic localized spin, the antinodal carriers may have a rather heavy effective mass, and thus may have a limited contribution in the

superfluid spectral weight n_s/m^*. Nodal charges are directly originating from doped holes, and known to support a rather high normal state conductivity, suggestive of a light mass. It looks as if the antinodal charges are helping the propagation of nodal pairs by creating large energy gaps, while the main superfluid spectral weight comes from the nodal pairs. This picture gives a natural explanation for n_s/m^* being nearly proportional to the doped (mobile) carrier concentration. Our model of coupled spin/charge operators suggests that the nodal and antinodal responses are strongly coupled, and cannot exist separately. Detailed roles and interplays of these two different regions of the Fermi surface are, however, yet to be clarified by future research.

D. retardation and phase diagram

In Fig. 3(b), we proposed the BE-BCS crossover region to have k_BT_F comparable to the energy of the pair mediating boson $\hbar\omega_B$ in a rather arbitrary discussion through the "retardation" concept. If we assume that the "optimal doping" region of the cuprates represents the crossover region, this argument suggests that $k_BT_F \sim 2,000$ K of the optimally doped YBCO could represent the energy scale of the pair mediating bosons. This crude estimate is consistent with spin fluctuations as a pair mediator [56], since $\hbar\omega_{AF}$ develops over the energy region up to the AF exchange interaction $J \sim 1,200 - 1,500$ K.

Furthermore, our argument of "resonant charge motion" can work only when the charge energy scale does not exceed the spin fluctuation energy scale. Doping further carriers in the overdoped region would increase the energy scale of doped normal holes exceeding the spin fluctuation energy scales. Then we cannot expect any more "resonant charge motion" nor "pairing mediated by spin fluctuations". This provides a reasoning from the microscopic model for why the crossover region appears at $k_BT_F \sim \hbar\omega_{AF}$, and why superconductivity in the overdoped region becomes progressively weaker with anomalous coexistence of paired and unpaired charges.

XI. DISCUSSIONS AND CONCLUSIONS

In our model, the closeness to the competing ground state can be a factor to reduce T_c (by reducing the resonance roton-minimum energy) and thus destructive to superconductivity, as well as a factor necessary to superconductivity in supplying mediating bosons in scattering and binding processes. This dual role of the competing ground state provides the very origin of the "dome like phase diagram", and also determines the distance of the maximum T_c from the T_{BE} line in Fig. 2. Although various different non-cuprate superconductors in Fig. 2 could have different "competing ground states", a similar situation might exist in most of the systems originating from Mott insulators, which could in the future provide some account of why their T_c is limited to an apparently universal maximum value of $T_c/T_F \sim 0.05$ in Fig. 2.

There have been two different schools of thought in explaining the superconductivity of cuprates. One assumes the condensation of pre-formed pairs in the underdoped region, which is somehow perturbed in the overdoped region. The other starts from "strong" superconductivity in the overdoped region and views it to be gradually destroyed with decreasing carrier density in the competition against other (presumably more magnetic) ground states in the underdoping region. Although still based on the former view point, the present picture qualitatively describes how to account for the effect of "competing ground states", and reconciles some conflict between these two views.

In theoretical discussions of HTSC or 1-dimensional systems, "spin-charge separation" is often the key underlying concept. Our model of charge propagation, in resonant with spin fluctuations, provides a new way out of the spin-charge separation problem and out of associated spin frustration. We pointed out several observations as evidence for extremely strong spin-charge coupling, which leads to the superconductivity of the cuprates. The strong involvement of the charge degrees of freedom in pairing could help interpretation of the isotope effect [85] and other signatures of lattice involvements, such as the "kink" in the electronic dispersion found in ARPES studies [86].

In summary, we have elucidated the role of superfluid density via accumulated μSR results and proposed the roton-like resonance mode as a primary determining factor of T_c. On the underdoped side, these two parameters, n_s/m^* and $\hbar\omega_{res}$ conspire to determine T_c, in a way very much similar to that in superfulid bulk ^{4}He. In the 214 system, close to competing ground states, the strong effect of reduced $\hbar\omega_{res}$ causes the early departure of the points in Fig. 1 from the nearly linear trend of other systems. We proposed a few new pictures including: 1) "hybrid spin-charge roton" to reconcile selection rules of neutron and Raman modes; 2) a microscopic model which explains how the charge motion and AF spin fluctuations can be coupled, in a sequential resonanting way, to create an attractive interaction among antinodal and nodal charges; 3) a possibility that the magnetic resonance mode plays a role of bonding bosons, analoguous to pi-mesons, which bind two nodal charges; and 4) the ARPES coherence peak and Raman $A1_g$ mode can be viewed as manifestations of the charge branch of the hybrid spin/charge roton. We also demonstrated the robustness of the superconductivity in the cuprates against spatial heterogeneity, analoguous to the superfluid He films, as an essential feature which cannot be expected in BCS superconductors. Hopefully, these pictures elucidate the fundamental importance of the BE condensation concept for the cuprates and provide useful conceptual frameworks for understanding their unique condensation and pairing aspects.

XII. ACKNOWLEDGMENT

The work at Columbia has been supported by the NSF DMR-0102752 INT-0314058 and CHE-0117752 (Nanoscale Science and Engineering Initiative). Some of the ideas in this paper were developed during the author's stay in IMR, Tohoku Univ., Japan, as a Visiting Professor during January - March, 2003. The author wishes to thank Profs. Bob Laughlin and Naoto Nagaosa for useful discussions. The author has had an intuitive view to interprete the magnetic resonance mode as a "roton-like" excitation for the past three years or so, based on the energy analogy shown in Fig. 6(b). When he confessed this idea as a wild speculation to these two scientists in the spring of 2003, they kindly pointed out several difficulties of this speculation. Struggles to resolve some of them led the author to develop the picture detailed in this paper. In various stages of the development of thoughts in this paper, discussions with Prof. Oleg Tchernyshyov were very illuminating. The preprint regarding the STM work of the 4 lattice-constant charge modulation, given by Prof. J.C. Seamus Davis, was also very useful.

[1] For general aspects and historical development of μSR, see Proceedings of nine international conferences on muon spin rotation / relaxation/ resonance in Hyperfine Interact. **6** (1979); **8** (1981); **17-19** (1984); **31** (1986); **63-65** (1990); **85-87** (1994); **104**-bf 106 (1997); Physica **B 289-290** (2000); and Physica **B** (Proceedings for μSR 2002, Williamsburg, Virginia, June, 2002), in press.

[2] For a general review of μSR, see, for example, A. Schenck, *Muon Spin Rotation Spectroscopy*, Adam Hilger, Bristol, 1985.

[3] For a recent reviews of μSR studies in topical subjects, see *Muon Science: Muons in Physics, Chemistry and Materials*, Proceedings of the Fifty First Scottish Universities Summer School in Physics, st. Andrews, August, 1988, ed. by S.L. Lee, S.H. Kilcoyne, and R. Cywinski, Inst. of Physics Publishing, Bristol, 1999.

[4] Y.J. Uemura, G.M. Luke, B.J. Sternlieb, J.H. Brewer, J.F. Carolan, W.N. Hardy, R. Kadono, J.R. Kempton, R.F. Kiefl, S.R. Kreitzman, P. Mulhern, T.M. Riseman, D.Ll. Williams, B.X. Yang, S. Uchida, H. Takagi, J. Gopalakrishnan, A.W. Sleight, M.A. Subramanian, C.L. Chien, M.Z. Cieplak, Gang Xiao, V.Y. Lee, B.W. Statt, C.E. Stronach, W.J. Kossler, and X.H. Yu, *Universal Correlations between T_c and n_s/m^* (Carrier Density over Effective Mass) in High-T_c Cuprate Superconductors*, Phys. Rev. Lett. **62** (1989) 2317.

[5] Y.J. Uemura, L.P. Le, G.M. Luke, B.J. Sternlieb, W.D. Wu, J.H. Brewer, T.M. Riseman, C.L. Seaman, M.B. Maple, M. Ishikawa, D.G. Hinks, J.D. Jorgensen, G. Saito, and H. Yamochi, *Basic Similarities among Cuprate, Bithmuthate, Organic, Chevrel-Phase and Heavy-Fermion Superconductors Shown by Penetration-Depth Measurements*, Phys. Rev. Lett. **66** (1991) 2665.

[6] Y.J. Uemura, *Energy Scales of Exotic Superconductors*, in *Polarons and Bipolarons in High-T_c Superconductors and Related Materials*, Proceedings of the International Workshop on Polarons and Bipolarons in High-T_c Superconductors and Related Materials, Cambridge, UK, April, 1994, ed. by E. Salje, A.S. Alexandrov and Y. Liang, Cambridge University Press (1995), p.p. 453-460.

[7] Y.J. Uemura, *Energy Scales of High-T_c Cuprates, Doped Fullerenes, and Other Exotic Superconductors*, Proceedings of International Symposium/Workshop on High-T_c Superconductivity and the C_{60} Family, May 1994, Beijing, ed., by H.C. Ren, Gordon and Breach (New York), (1995), p.p. 113-142.

[8] B. Nachumi, A. Keren, K. Kojima, M. Larkin, G.M. Luke, J. Merrin, O. Tchernyshov, Y.J. Uemura, N. Ichikawa, M. Goto, and S. Uchida, *Muon Spin Relaxation Studies of Zn-Substitution Effects in High-T_c Cuprate Superconductors*, Phys. Rev. Lett. **77** (1996) 5421.

[9] S.H. Pan, E.W. Hudson, K.M. Lang, H. Eisaki, S. Uchida, J.C. Davis, *Imaging the Effects of Individual Zinc Impurity Atoms on Superconductivity in $Bi_2Sr_2CaCu_2O_{8+\delta}$*, Nature (London) **403** (2000) 746.

[10] K.M. Lang, V. Madhavan, J.E. Hoffman, E.W. Hudson, H. Eisaki, S. Uchida, J.C. Davis *Imaging the granular structure of high-Tc superconductivity in underdoped $Bi_2Sr_2CaCu_2O_{8+\delta}$* Nature (London) **415** (2002) 412 - 416.

[11] K. McElroy, D.-H. Lee, J.E. Hoffman, K.M. Lang, J. Lee, E.W. Hudson, H. Eisaki, S. Uchida, J.C. Davis, *Detection of heterogeneous charge order coexisting with homogeneous nodal superconductivity in strongly underdoped $Bi_2Sr_2CaCu_2O_{8+\delta}$*, cond-mat/0404005.

[12] J. Corson, R. Mallozzi, J. Orenstein, J.N. Eckstein, I. Bozovic, *Vanishing of phase coherence in underdoped $Bi_2Sr_2CaCu_2O_{8+\delta}$*, Nature (London) **398** (1999) 221.

[13] Z.A. Xu, N.P. Ong, Y. Wang, T. Kakeshita, S. Uchida, *Vortex-like excitations and the onset of superconducting phase fluctuation in underdoped $La_{2-x}Sr_xCuO_4$*, Nature **406** (2000) 486.

[14] Y. Wang, S. Ono, Y. Onose, G. Gu, Y. Ando, Y. Tokura, S. Uchida, and N. P. Ong, *Dependence of Upper Critical Field and Pairing Strength on Doping in Cuprates*, Science **299** (2003) 86.

[15] H.A. Mook, M. Yethiraj, G. Aepli, T.E. Mason, T. Armstrong, *Polarized Neutron Determination of Magnetic Excitations in $YBa_2Cu_3O_7$*, Phys. Rev. Lett. **70** (1993) 3490.

[16] H.F. Fong, B. Keimer, D. Reznik, D.L. Milius and I.A. Aksay, *Polarized and unpolarized neutron-scattering study of the dynamic spin susceptibility of $YBa_2Cu_3O_7$*, Phys. Rev. **B54** (1996) 6708.

[17] P. Bourges, Y. Sidis, H.F. Fong, L.P. Regnault, J. Bossy, A. Ivanov, B. Keimer, *The spin excitation spectrum in superconducting $YBa_2Cu_3O_{6.85}$*, Science **288** (2000) 1234.

[18] Y. Sidis, S. Pailhés, B. Keimer, P. Bourges, C. Ulrich, L.P. Regnault, *Magnetic resoanant excitation in high-T_c superconductors*, cond-mat/0401328.

[19] Y. Gallais, A. Sacuto, P. Bourges, Y. Sidis, A. Forget and D. Colson, *Evidence for Two Distinct Energy Scales in the Raman Spectra of $YBa_2(Cu_{1-x}Ni_x)_3O_{6.95}$*, Phys. Rev. Lett. **88** (2002) 177401, and references therein.

[20] O.V. Misochko and G. Gu, *electronic Raman scattering in disordered $Bi_2Sr_2Ca(Cu_{1-y}Fe_y)_2O_\delta$: impurity scattering*

effects, Phys. Rev. **B59** (1999) 11183.

[21] L.V. Gasparov, P. Lemmens, M. Brinkmann, N.N. Kolesnikov, G. Günterodt, *Electronic Raman scattering in the single CuO_2 lyered superconductor $Ta_2Ba_2CuO_{6+\delta}$*, Phys. Rev. **B55** (1997) 1223.

[22] X.K. Chen, J.C. Irwin, H.J. Trodahl, T. Kimura and K. Kishio, *Investigation of the Superconducting Gap in $La_{2-x}Sr_xCuO_4$ by Raman Spectroscopy*, Phys. Rev. Lett. **73** (1994) 3290.

[23] D.L. Feng, D.H. Lu, K.M. Shen, C. Kim, H. Eisaki, A. Damascelli, R. Yoshizaki, J. Shimoyama, K. Kishio, G.D. Gu, S. Oh, A. Andrus, J. O'Donnell, J.N. Eckstein, Z.X. Shen, *Signature of superfluid density in the single-particle excitation spectrum of $Bi_2Sr_2CaCu_2O_{8+\delta}$*, Science **289** (2000) 277.

[24] Y.J. Uemura, A. Keren, L.P. Le, G.M. Luke, W.D. Wu, Y. Kubo, T. Manako, Y. Shimakawa, M. Subramanian, J.L. Cobb, and J.T. Markert, *Magnetic Field Penetration Depth in $Tl_2Ba_2CuO_{6+\delta}$ in the Overdoped Regime*, Nature (London) **364** (1993) 605.

[25] A.T. Savici, Y. Fudamoto, I.M. Gat, T. Ito, M.I. Larkin, Y.J. Uemura, G.M. Luke, K.M. Kojima, Y.S. Lee, M.A. Kastner, R.J. Birgeneau, K. Yamada, *Muon spin relaxation studies of incommensurate magnetism and superconductivity in stage-4 $La_2CuO_{4.11}$ and $La_{1.88}Sr_{0.12}CuO_4$*, Phys. Rev. **B66** (2002) 014524.

[26] K.M. Kojima, S. Uchida, Y. Fudamoto, I.M. Gat, M.I. Larkin, Y.J. Uemura, G.M. Luke, *Superfluid density and volume fraction of static magnetism in stripe-stabilized $La_{1.85-y}Eu_ySr_{0.15}CuO_4$*, Physica **B 36** (2003) 316-320.

[27] C.L. Seaman, J.J. Neumeier, M.B. Maple, L.P. Le, G.M. Luke, B.J. Sternlieb, Y.J. Uemura, J.H. Brewer, R. Kadono, R.F. Kiefl, S.R. Kreitzman, T.M. Riseman, *Magnetic penetration depth of $Y_{1-x}Pr_xBa_2Cu_3O_{6.97}$ measured by muon-spin relaxation*, Phys. Rev. **B42** (1990) 6801.

[28] B. Pümpin, H. Keller, W. Kündig, I.M. Savić, J.W. Schneider, H. Simmer, P. Zimmermann, E. Kaldis, S. Rusiecki, C. Rossel, *μSR in oxygen deficient $YBa_2Cu_3O_x$ ($6.5 \leq x \leq 7.0$)*, Hyperfine Interact. **63** (1990) 25.

[29] J.L. Tallon, C. Bernhard, U. Binninger, A. Hofer, G.V.M. Williams, E.J. Ansaldo, J.I. Budnick, Ch. Niedermayer, *In-Plane Anisotropy of the Penetration Depth Due to Superconductivity on the Cu-O Chains in $YBa_2Cu_3O_{7-\delta}$, $Y_2Ba_4Cu_7O_{15-\delta}$, and $YBa_2Cu_4O_8$* Phys. Rev. Lett. **74** (1995) 1008.

[30] Ch. Niedermayer, C. Bernhard, U. Binninger, H. Glückler, J.L. Tallon, E.J. Ansaldo, and J.I. Budnick, *Muon Spin Rotation Study of the Correlation Between T_c and n_s/m^* in Overdoped $Tl_2Ba_2CuO_{6+\delta}$*, Phys. Rev. Lett. **71** (1993) 1764.

[31] A. Keren, A. Kanigel, J.S. Lord, A. Amato, *Superconductivity and magnetism in $(Ca_xla_{1-x})(Ba_{1.75-x}La_{0.25+x})Cu_3O_y$: a μSR investigation*, Solid State Commun. **126** (2003) 39.

[32] J. Bardeen, L.N. Cooper and J.R. Schrieffer, *Theory of Superconductivity*, Phys. Rev. **108** (1957) 1175.

[33] Y.J. Uemura, *Superfluid density of high-T_c cuprate systems: implication on condensation mechanisms, heterogeneity and phase diagrams*, Solid State Commun. **126** (2003) 23-38; erratum *ibid* 425.

[34] W. Barford and J.M.F. Gunn, *The theory of the measurements of the London penetration depth in uniaxial type-II superconductors by muon spin rotation*, Physica **C156** (1988) 515.

[35] Y.J. Uemura, A. Keren, G.M. Luke, L.P. Le, B.J. Sternlieb, W.D. Wu, J.H. Brewer, R.L. Whetten, S.M. Huang, Sophia Lin, R.B. Kaner, F. Diederich, S. Donnovan, G Grüner, K. Holczer, *Magnetic Field Penetration Depth in K_3C_{60} Measured by Muon Spin Relaxation*, Nature **352** (1991) 605.

[36] Y.J. Uemura, A. Keren, L.P. Le, G.M. Luke, W.D. Wu, J.S. Tsai, K. Tanigaki, K. Holczer, S. Donovan, R.L. Whetten, *System Dependence of the Magnetic-field Penetration Depth in C_{60} Superconductors*, Physica **C235-240** (1994) 2501.

[37] L.P. Le, G.M. Luke, B.J. Sternlieb, W.D. Wu, Y. J. Uemura, J.H. Brewer, T.M. Riseman, C. E. Stronach, G. Saito, H. Yamochi, H.H. Wang, A.M. Kini, K.D. Carlson, J.M. Williams *Muon-spin-relaxation measurements of magnetic penetration depth in organic superconductors (BEDT-TTF)$_2$-X: X=Cu(NCS)$_2$ and Cu[N(CN)$_2$]Br* Phys. Rev. Lett. **68**, (1992) 1923.

[38] Y.J. Uemura, Y. Fudamoto, I.M. Gat, M.I. Larkin, G.M. Luke, J. Merrin, K.M. Kojima, K. Itoh, S. Yamanaka, R.H. Heffner, D.E. MacLaughlin, *μSR Studies of Intercalated HfNCl Superconductors*, Physica **B289** (2000) 389.

[39] Y.J. Uemura, P.L. Russo, A.T. Savici, C.R. Wiebe, G.J. MacDougall, G.M. Luke, M. Mochizuki, Y. Yanase, M. Ogata, M.L. Foo, R.J. Cava, *Unconventional superconductivity in $Na_{0.35}CoO_2{\cdot}1.3D_2O$ and proximity to a magnetically ordered phase*, cond-mat/0403031.

[40] C.A. Regal, M. Greiner, D.S. Jin, *Observation of Resonance Condensation of Fermionic Atom Pairs*, Phys. Rev. Lett. **92** (2004) 040403.

[41] P. Nozières and S. Schmitt-Rink, *Bose condensation in an attractive Fermion Gas - From weak to strong coupling superconductivity* J. Low Temp. Phys. **59** (1985) 195.

[42] H. Alloul, T. Ohno, and P. Mendels, *^{89}Y NMR evidence for a fermi-liquid behavior in $YBa_2Cu_3O_{6+x}$*, Phys. Rev. Lett. **63** (1989) 1700-1703.

[43] M. Takigawa, A.P. Reyes, P.C. Hammel, J.D. Thompson, R.H. Heffner, Z. Fisk, K. C. Ott, *Cu and O NMR studies of the magnetic properties of $YBa_2Cu_3O_{6.63}$ (Tc=62 K)*, Phys. Rev. **B43** (1991) 247-257.

[44] T. Ito, H. Takagi, T. Ido, S. Ishibashi, S. Uchida, *Normal state conductivity between CuO_2 planes in copper-oxide superconductors*, Nature **350** (1991) 596.

[45] V. Emery and S. Kivelson, *Importance of phase fluctuations in superconductors with small superfluid density*, Nature **374** (1995) 434.

[46] J.M. Kosterlitz and D.J. Thouless, *Ordering, Metastability and Phase-Transitions in 2-Dimensional Systems*, J. Phys. **C: Solid State Phys. 6**, (1973) 1181

[47] R. Friedberg and T.D. Lee *Gap energy and long-range order in the boson-fermion model of superconductivity*, Phys. Rev. **B40** (1989) 6745.

[48] R. Friedberg, T.D. Lee, H.C. Ren, *Applicatin of the s-channel theory to the μSR and Hall number experiments on high-T_c superconductors*, Physics Letters **A152** (1991) 423.

[49] M. Randeria, *Crossover from BCS theory to Bose-Einstein Condensation*, in *Bose-Einstein Condensation*, ed. by A. Griffin, D.W. Snoke, S. Stringari, Cambridge University Press, Cambridge, 1995, p.p. 355-391, and references therein.

[50] S. Uchida, *Critical points in the cuprate phase diagram*, Solid State Commun. **126** (2003) 57.

[51] G. Agnolet, D.F. McQueeney, J.D. Reppy, *Kosterlitz-*

Thouless Transition in Helium Films, Phys. Rev. **B39** (1989) 8934.

[52] Y.J. Uemura *et al.*, B.J. Sternlieb, D.E. Cox, V.J. Emery, A.R. Moodenbaugh, M. Suenaga, J.H. Brewer, J.F. Carolan, W.N. Hardy, R. Kadono, J.R. Kempton, R.F. Kiefl, S.R. Kreitzman, G.M. Luke, P. Mulhern, T.M. Riseman, D.Ll. Williams, B.X. Yang, W.J. Kossler, X.H. Yu, H.E. Shoene, C.E. Stronach, J. Goparakrishnan, M.A. Subramanian, A.W. Sleight, H.R. Hart, K.W. Ley, H. Takagi, S. Uchida, Y. Hidaka, T. Murakami, S. Etemad, P. Barboux, D. Keane, V.Y. Lee, D.C. Johnston, *μSR Studies on High-T_c Superconductivity*, J. Physique (Paris) Colloque **49**, C8:2087-C8:2092 (1988).

[53] J.E. Sonier, J.H. Brewer, R.F. Kiefl, *μSR Studies of the Vortex State in Type-II Superconductors*, Rev. Mod. Phys. **72** (2002) 769.

[54] D.J. Bishop, J.E. Berthold, J.M. Parpia, J.D. Reppy, *Superfluid Density of Thin ^{4}He Films Adsorbed in Porous Vicor Glass*, Phys. Rev. **B24** (1981) 5047.

[55] H. Chyo and G.A. Williams, *Superfluid Phase Transition of ^{3}He-^{4}He Mixture Films Adsorbed on Alumina Powder*, J. Low Temp. Phys. **110** (1998) 533.

[56] Y.J. Uemura, *Bose-Einstein to BCS Crossover Picture for High-T_c Cuprates* Physica **C282-287** (1997) 194-197.

[57] D.J. Bishop and J.D. Reppy, *Study of superfluid transition in 2-dimensional He-4 films*, Phys. Rev. Lett. **40** (1978) 1727.

[58] Ø. Fisher, J.M. Triscone, O. Brunner, L. Antognazza, M. Affronte, O. Eibt, L. Mi/'eville, T. Boichat, M.G. Karkut, *Superconductivity in artificially grown copper-oxide superlattices*, Physics **B169** (1991) 116.

[59] V.C. Aguilera-Navarro, M. de Llano, M.A. Solis, *Bose-Einstein condensation for general dispersion relations*, Eur. J. Phys. **20** (1999) 177.

[60] D.G. Henshaw and A.D.B. Woods, *Modes of Atomic Motions in Liquid Helium by Inelastic Scattering of Neutrons*, Phys. Rev. **121** (1961) 1266.

[61] O.W. Dietrich, E.H. Graf, C.H. Huang, L. Passell, *Neutron scattering by rotons in liquid helium*, Phys. Rev. **A5** (1972) 1377.

[62] N.B. Christensen, D.F. McMorrow, H.M. Rønnow, B. Lake, S. Hayden, G. Aeppli, T.G. Perring, M. Mangkorntong, M. Nohara, H. Takagi, *Universal dispersive excitations in the high-temperature superconductors*, cond-mat/0403439.

[63] M.R. Norman and C. Pepin, *The electronic nature of high temperature cuprate superconductors*, cond-mat/0302347.

[64] M. Eschrig and M.R. Norman, *Effect of the magnetic resonance on the electronic spectra of high-Tc superconductors*, Phys. Rev. **B67** (2003) 144503.

[65] F. Onufrieva and P. Pfeuty, *Spin dynamics of a two dimensional metal in a superconducting state: application to the high-T_c cuprates*, Phys. Rev. **B65** (2002) 054515, and references therein.

[66] S.M. Girvin, A.H. MacDonald, P.M. Platzman, *Magneto-roton theory of collective excitations in the fractional quantum Hall effect*, Phys. Rev. **B33** (1986) 2481.

[67] T.J. Greytak, R. Woerner, J. Yan, R. Benjamin, *Experimental evidence for a two-roton bound state in superfluid helium*, Phys. Rev. Lett. **25** (1970) 1547.

[68] M. Vershinin, S. Misra, S. Ono, Y. Abe, Y. Ando, A. Yazdani, *Local Ordering in the Pseudogap State of the High-Tc Superconductor $Bi_2Sr_2CaCu_2O_{8+\delta}$*, Science **303** (2004) 1995-1998.

[69] T. Hanaguri, C. Lupien, Y. Kohsaka, D.-H. Lee, M. Azuma, M. Takano, H. Takagi, J.C. Davis, *Discovery of a "checkerboard" electronic crystal phase in the lightly doped Mott insulator $Ca_{2-x}Na_xCuO_2Cl_2$*, preprint (2004).

[70] H.C. Fu, J.C. Davis, D.H. Lee, *On the Charge Ordering Observed by Recent STM Experiments*, cond-mat/0403001.

[71] Z. Nazario and D.I. Santiago, *Roton Induced Modulations in Underdoped Cuprates as a Signature of Incipient Electronic Order*, cond-mat/0403374.

[72] J.M. Tranquada, B.J. Sternlieb, J.D. Axe, Y. Nakamura, S. Uchida, *Evidence for stripe correlations of spins and holes in copper-oxide superconductors*, Nature **375** (1995) 561.

[73] C.C. Homes, D.A. Bonn, R. Liang, W.N. Hardy, D.N. Basov, T. Timusk, and B.P. Clayman *Effect of Ni impurities on the optical properties of $YBa_2Cu_3O_{6+y}$* Phys. Rev. **B60** (1999) 9782-9792.

[74] J.W. Loram, K.A. Mirza, J.M. Wada, J.R. Cooper, W.Y. Liang, *The electronic specific heat of cuprate superconductors*, Physica **C235-240** (1994) 134.

[75] C. Bernhard, J.L. Tallon, Th. Blasius, A. Golnik, Ch. Niedermayer, *Anomalous Peak in the Superconducting Condensate Density of Cuprate High-T_c Superconductors at a Unique Doping State*, Phys. Rev. Lett. **86** (2001) 1614.

[76] J. Hofer, J. Karpinski, M. Willemin, G.I. Meijer, E.M. Kopnin, R. Molinski, H. Schwer, C. Rossel, and H. Keller *Doping dependence of superconducting parameters in $HgBa_2CuO_{4+d}$ single crystals*, Physica **C297** (1998) 103-110.

[77] J. Schützmann, S. Tajima, S. Miyamoto, S. Tanaka, *c-Axis Optical Response of Fully Oxygenated $YBa_2Cu_3O_{7-\delta}$: Observation of Dirty-Limit-Like Superconductivity and Residual Unpaired Carriers*, Phys. Rev. Lett. **73** (1994) 174.

[78] N. Gedik and J. Orenstein, private communication (2004).

[79] Y.J. Uemura, *Microscopic phase separation in the overdoped region of high-T_c cuprate superconductors*, Solid State Commun. **120** (2001) 347.

[80] J.L. Tallon and J.W. Loram, *The doping dependence of T^* – what is the real high-T_c phase diagram ?*, Physica **C349** (2001) 53.

[81] J. Hwang, T. Timusk and G.D. Gu, *High-transition-temperature superconductivity in the absence of the magnetic resonance mode*, Nature **427** (2004) 715.

[82] T. Timusk and B. Statt, *The pseudogap in high temperature superconductors: an experimental survey*, Rep. Prog. Phys. **62** (1999) 61.

[83] Y. Wang, Z.A. Xu, T. Kakeshita, S. Uchida, S. Ono, Y. Ando, N.P. Ong, *Onset of the vertexlike Nernst signal above T_c in $La_{2-x}Sr_xCuO_4$ and $Bi_2Sr_{2-y}La_yCuO_6$*, Phys. Rev. **B64** (2001) 224519.

[84] S. Inouye, M.R. Andrews, J. Stenger, H.J. Miesner, D.M. Stamper-Kurn, W. Ketterle, *Observation of Feshbach resonances in a Bose-Einstein condensate*, Nature **392** (1998) 151.

[85] R. Khasanov, A. Shengelaya, E. Morenzoni, K. Conder, I.M. Savić, H. Keller, *Oxygen-isotope effect on the in-plane penetration depth in cuprate superconductors*, cond-mat/0404428.

[86] A. Damascelli, Z. Hussain, Z.X. Shen, *Angle-resolved photoemission studies of the cuprate superconductors*, Rev. Mod. Phys. **75** (2003) 473.

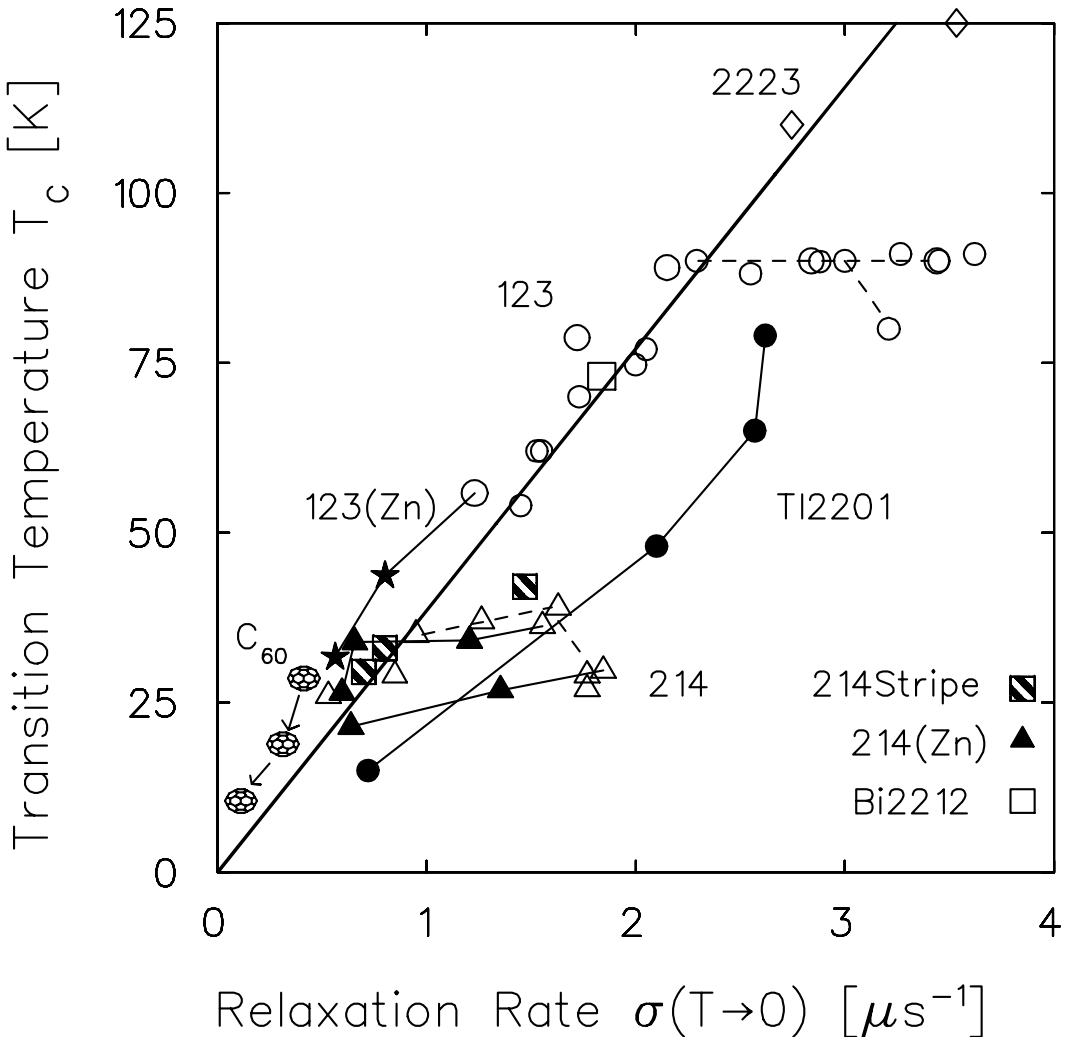

FIG. 1: Muon spin relaxation rate $\sigma \propto n_s/m^*$ at $T \rightarrow 0$ from various high-T_c cuprate superconductors [4,5,8,24-27] and A_3C_{60} systems [35,36] plotted against the superconducting transition temperature T_c. The points for HTSC with open symbols represent simple hole doped systems, while closed triangles are for (Cu,Zn) substitution [8], "stripe" symbols for systems with formation of island regions with incommensurate static spin modulations [25], and closed circles for overdoped Tl2201.

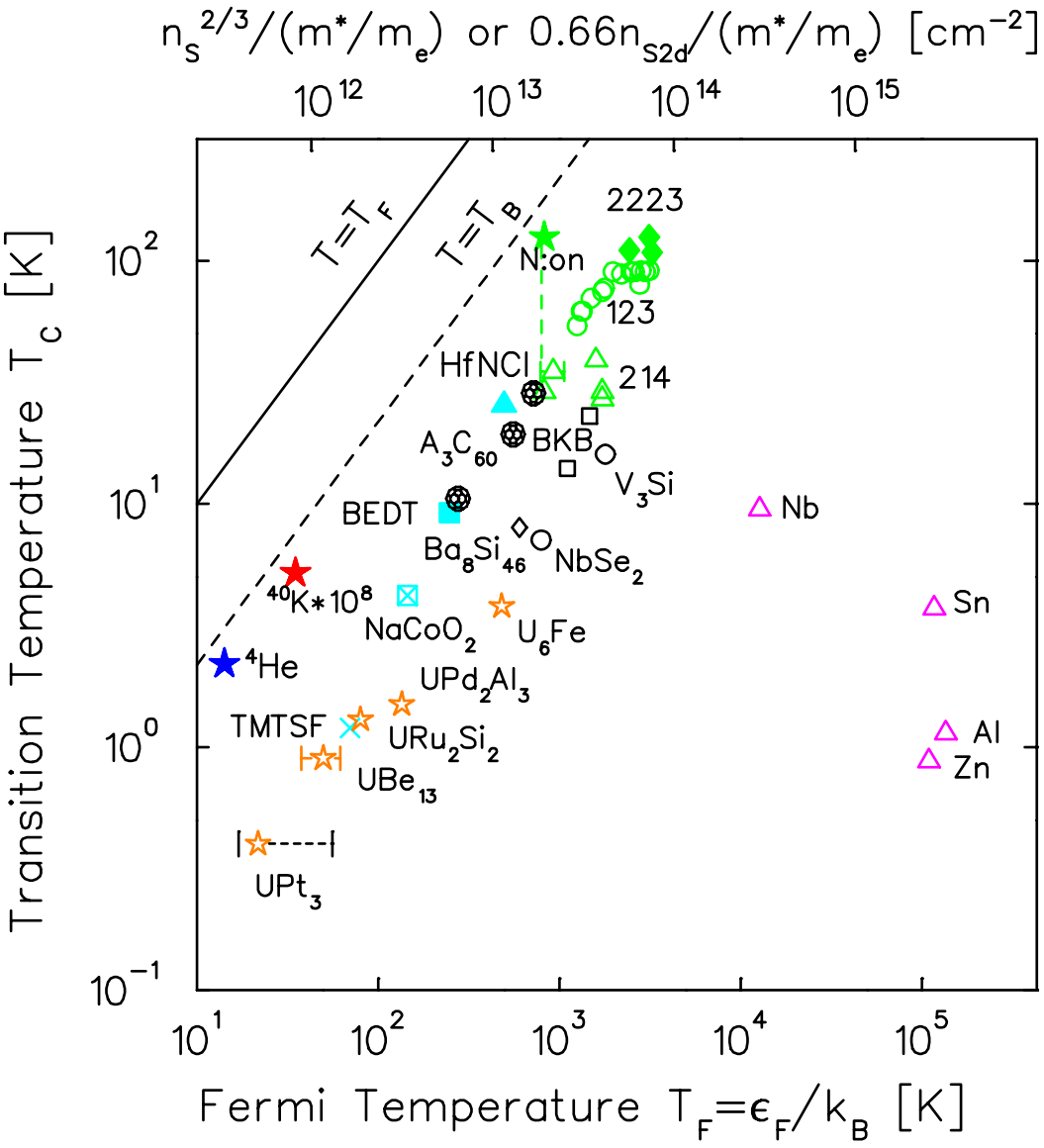

FIG. 2: Plot of T_c versus the effective Fermi temperature T_F obtained from the superfluid response n_s/m^* of various superconducting systems, first attempted in ref. [5] in 1991, and updated including results from refs [4,5,35-39]. We see an empirical upperlimit $T_c/T_F \sim 0.05$ for superconducting systems. Also included are the corresponding points for the superfluid ^{4}He (blue star) and the ultracold ^{40}K [40] in the BE-BCS crossover region (red star; with T_c and T_F both multiplied by 10^8). The T_B line shows the BE condensation temperature for the ideal bose gas of boson density $n_s/2$ and mass $2m^*$. The green star represents the onset temperature T_{on} of the Nernst effect, shown in Fig. 8(b), for $La_{1.9}Sr_{0.1}CuO_4$ [13,14], which represents the case for "hypothetical 3-d and roton-less underdoped LSCO".

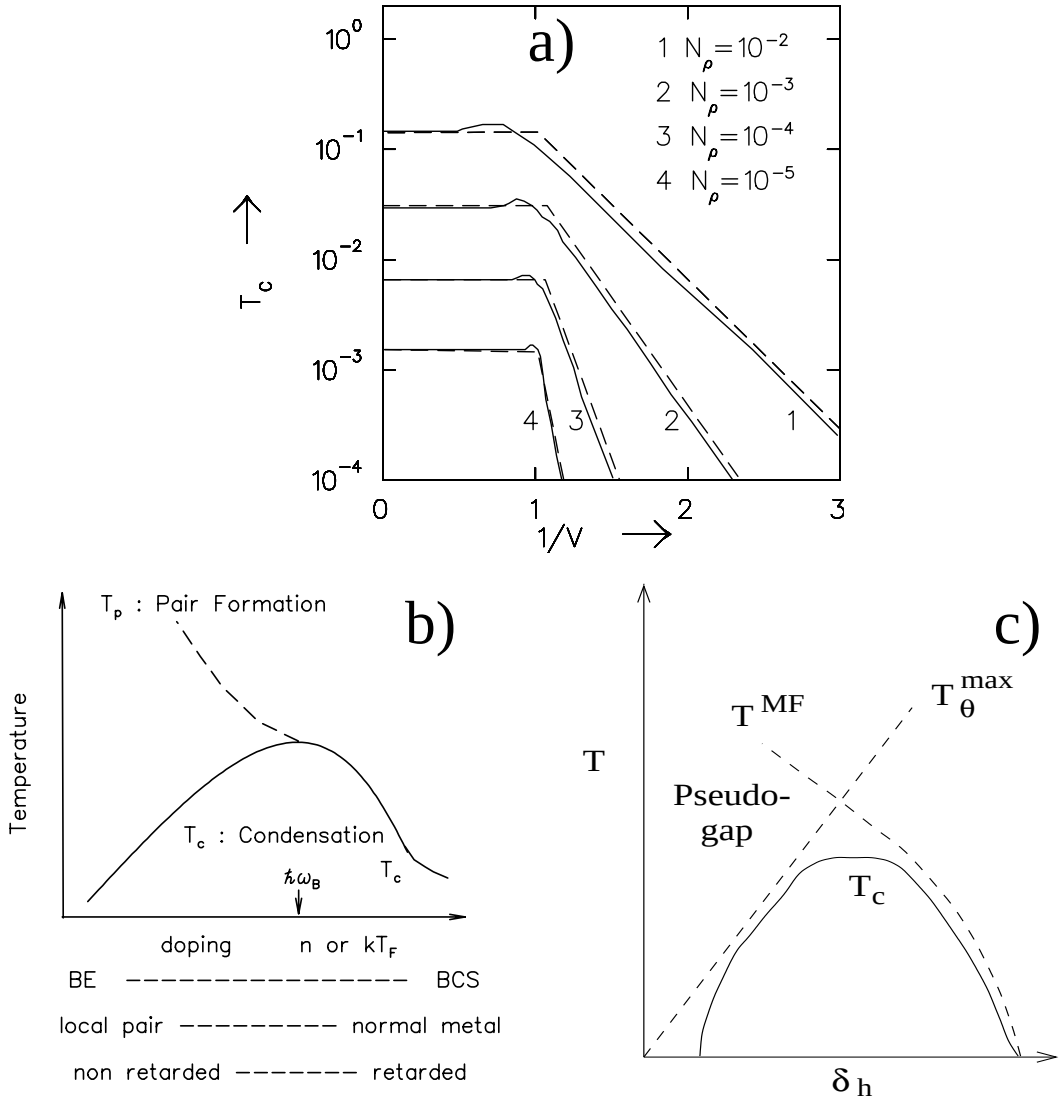

FIG. 3: (a) Transition temperature T_c plotted against inverse of the normalized attractive coupling strength V in the BE-BCS crossover region obtained by Nozières and Schmitt-Rink [41] in 1984 for various particle densities. Since V is defined with parameters including N_p, the N_p dependence for fixed interaction strength cannot be directly obtained from this figure. (b) The BE-BCS crossover picture proposed by Uemura [6,7] in 1994 with the crossover region characterized by the matching of kinetic energy $k_B T_F$ of the condensing carriers with the mediating boson energy $\hbar\omega_B$. When one identifies the pair formation temperature T_p as the pseudo-gap temperature T^*, this phase diagram can be mapped to the case of HTSC. (c) A phase diagram based on the superconducting phase fluctuations in the pseudogap region proposed by Emery and Kivelson [45] in 1995 as an explanation to the relationship shown in Fig. 1. T^{MF} represents the mean-field attractive interaction, while the T_Θ^{max} shows the maximum temperature up to which the superconductivity in 2-d systems can survive against thermal excitations of phase fluctuations.

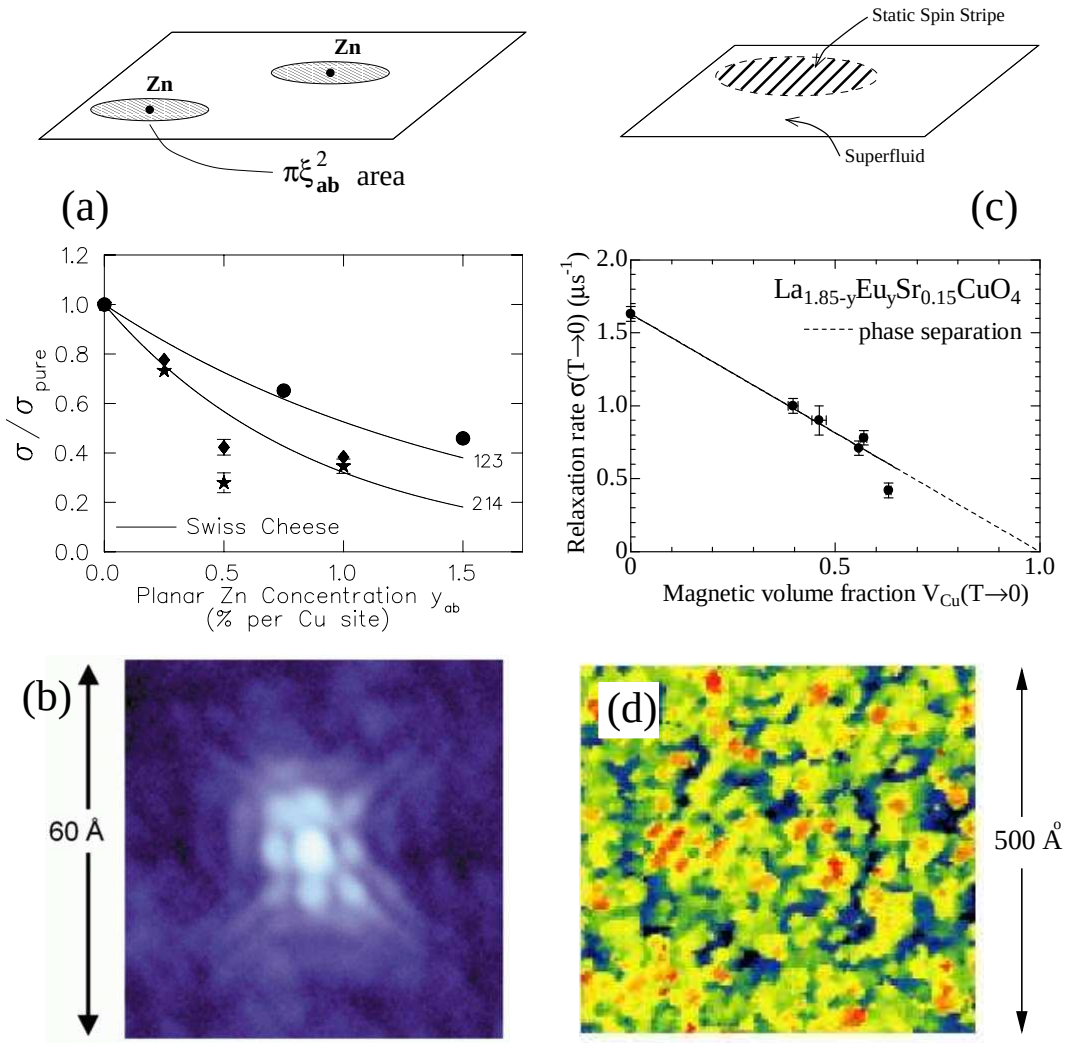

FIG. 4: (a) Muon spin relaxation rate $\sigma(T \rightarrow 0) \propto n_s/m^*$ plotted against the planar Zn concentration in the (Cu,Zn) substituted $YBa_2Cu_3O_{6.63}$ (123) and $La_{2-x}Sr_x(Cu,Zn)O_4$ with $x = 0.15$ and 0.20 [8]. The solid line represents the variation expected for the "swiss cheese model" illustrated on the top, where superconductivity around each Zn is assumed to be destroyed in the area of $\pi\xi_{ab}^2$. (b) The gapped response (blue color) versus normal state density of states (white color) detected around one Zn impurity in (Cu,Zn) substituted Bi2212 by STM [9]. (c) Muon spin relaxation rate $\sigma(T \rightarrow 0) \propto n_s/m^*$ in Eu substituted $(La,Eu)_{1.85}Sr_{0.15}CuO_4$ plotted against the volume fraction V_{Cu} of Cu moments having static magnetic order [26]. The results demonstrate the trade off between superconducting and magnetic volume fractions, expected in the "magnetic island formation" illustrated at the top. (d) The "gap-map" obtained by STM in moderately underdoped Bi2212 [10,11]. The red-yellow regions represent the area where the sharp superconducting gap is observed, while blue and black region has a response similar to those found in the "pseudogap" region [68] or the nonsuperconducting very underdoped region [69]. The characteristic length scale for this spontaneous formation of spatial heterogeneity is comparable to the coherence length ξ_{ab}.

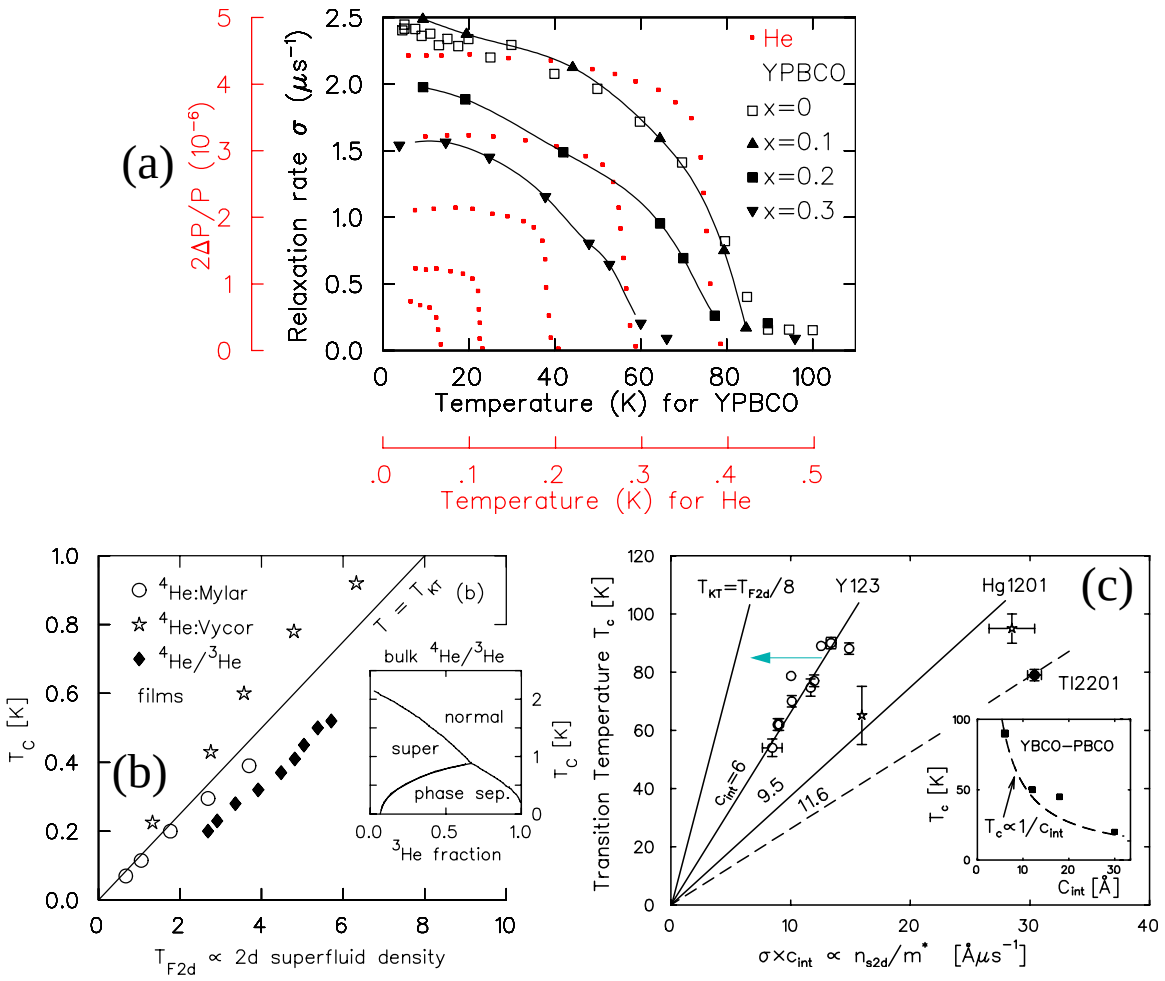

FIG. 5: (a) Temperature dependences of the superfluid responses in the thin-film of ^{4}He adsorbed on Mylar films (red points and axes) [51] compared with those in $(Y_{1-x}Pr_x)Ba_2Cu_3O_7$ observed by μSR in unoriented [27] and oriented (multiplied with 1/1.4) [52] ceramic specimens. The solid lines are guides to the eye. (b) The superfluid transition temperature T_c versus the 2-d superfluid density at $T \to 0$ for ^{4}He films on regular (Mylar) [51] and porous (Vycor) [54] media, and ^{4}He/^{3}He mixture films adsorbed on fine alumina powders [55] where the bulk phase separation in the inset figure is changed to microscopic heterogeneity via porous/powder media. The linear line represents values of superfluid density jump expected at $T = T_c$ from the Kosterlitz-Thouless theory [46]. (c) T_c plotted against the 2-d superfluid density $n_{s2d}/m^* \propto \sigma(T \to 0) \times c_{int}$ for various cuprate systems having different average interlayer spacing c_{int} [56]. The inset figure shows the T_c variation against c_{int} in MBE $YBa_2Cu_3O_7$ films where non-superconducting $PrBa_2Cu_3O_7$ was sandwiched with every unit cell along the c-axis direction [58]. The blue arrow illustrates the reduction of the superfluid density from the $T \to 0$ value towards the value expected at T_{KT}. The YBCO data in (a) shows even further reduction from this "T_{KT} jump" [57] value as the T_c is approached.

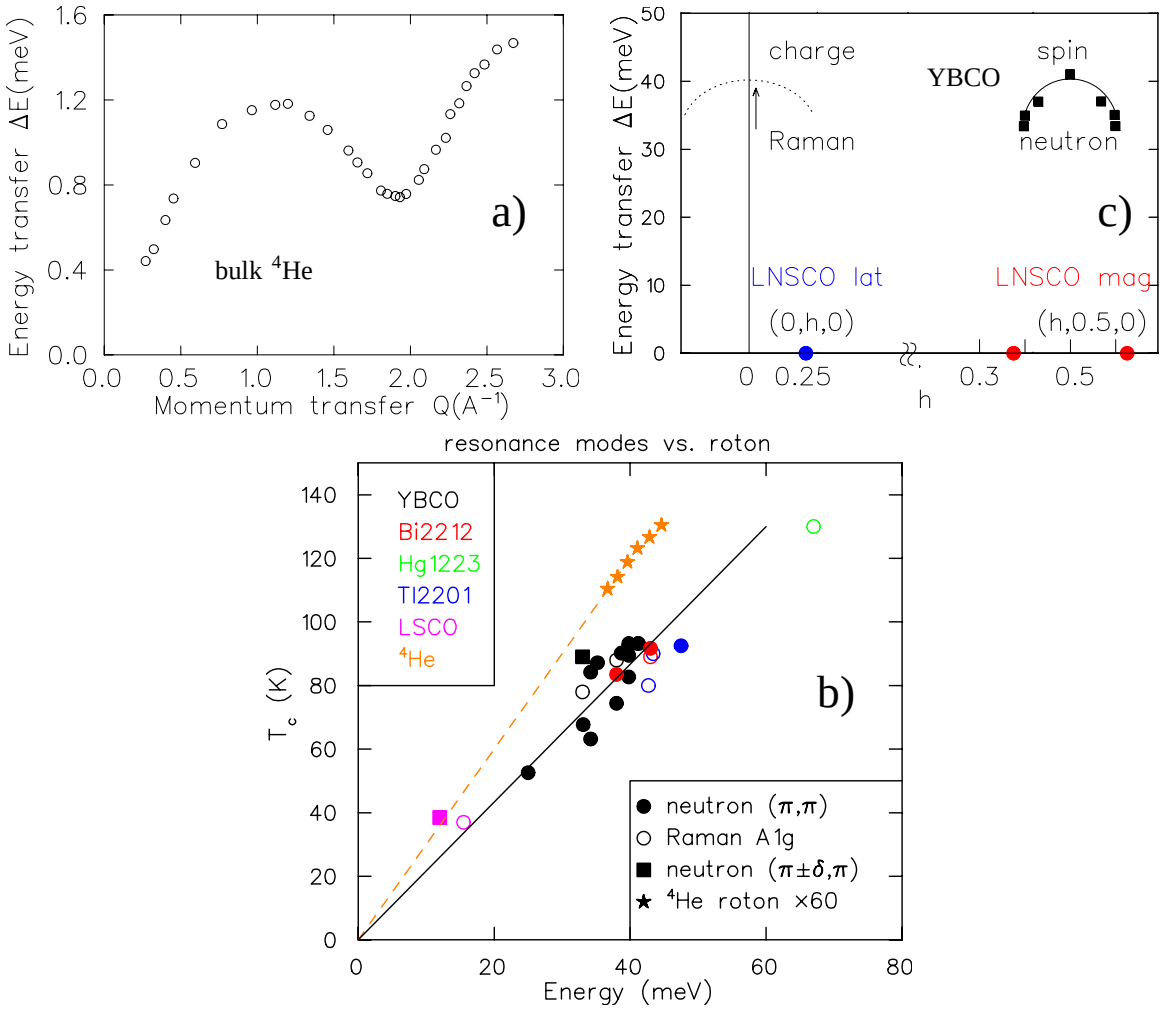

FIG. 6: (a) The dispersion relation of phonon-roton excitations in superfluid ^{4}He observed by neutron scattering [60]. (b) The plot of T_c versus energy of the roton minimum of bulk superfluid ^{4}He (values for both axes multiplied by a factor 60) measured under applied pressures [61], compared with the relationship seen in HTSC systems for the energies of the neutron resonance mode at (π,π) [15-18] and the Raman A1$_g$ mode [19-22]. Also included are the neutron energy transfers at the $(\pi \pm \delta, \pi)$ point in YBCO [17] and LSCO [62]. (c) The dispersion relation around the (π,π) resonance mode observed in YBCO by neutrons [17] (closed circles), the location of the satellite Bragg peaks (red = magnetic; blue = lattice, estimated from the adjacent Brillouin zone) found in the static spin/charge stripe system (La,Nd,Sr)$_2$CuO$_4$ (LNSCO) [72], and the proposed charge branch of the hybrid spin/charge roton (dotted line), to which the Raman A1$_g$ response in (b) is ascribed.

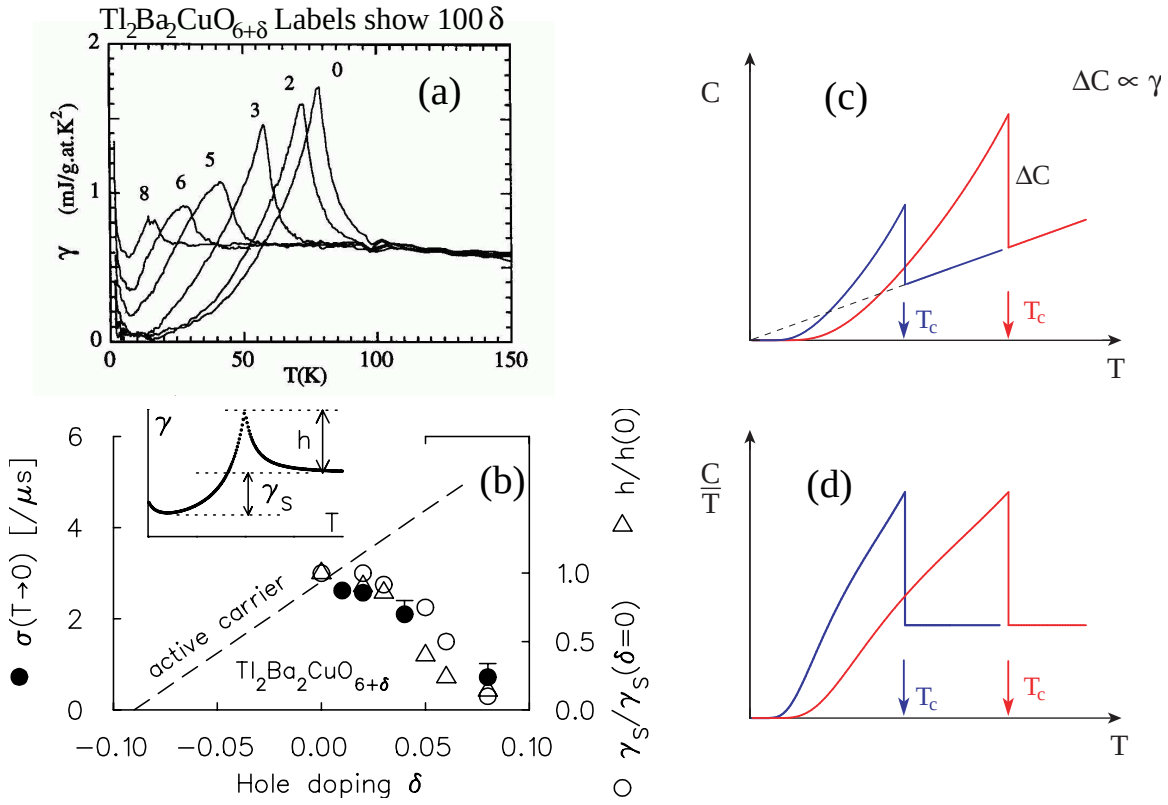

FIG. 7: (a) The electronic specific heat observed by Loram *et al.* [74] in the overdoped Tl2201 systems. (b) The variation of the μSR relaxation rate $\sigma(T \to 0)$ in Tl2201 [24] compared with the "gapped" response γ_S (open circles) and the peak height h (open triangles) from the data in (a). (c) The specific heat jump in standard BCS superconductors with different T_c's. (d) Same as (c) but plotted as $\gamma = C/T$, to be compared to (a). Figures (a)-(d) together provide strong evidence for phase separation in the overdoped cuprates developing with increasing overdoping.

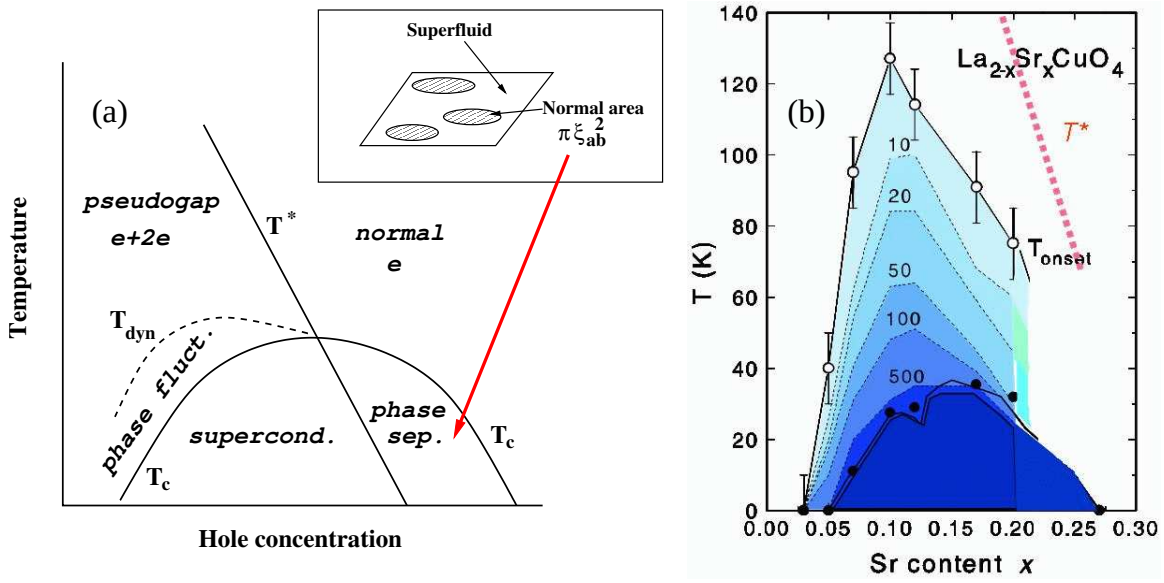

FIG. 8: (a) A generic phase diagram proposed for cuprates by Uemura [33], including the distinction between the pair formation T^* and the onset temperature of dynamic superconductivity T_{dyn} which corresponds to the T_{onset} of the Nernst effect. The inset illustrates the proposal of microscopic phase separation between superconducting and normal metal regions in the overdoped region [79]. (b) The region of the Nernst effect, shown in the T-x phase diagram for LSCO [83]. The result of T_{onset} for the $x = 0.10$ sample is plotted with the green star symbol in Fig. 2. The T^* values shown by the red-dashed line are taken from ref. [82].

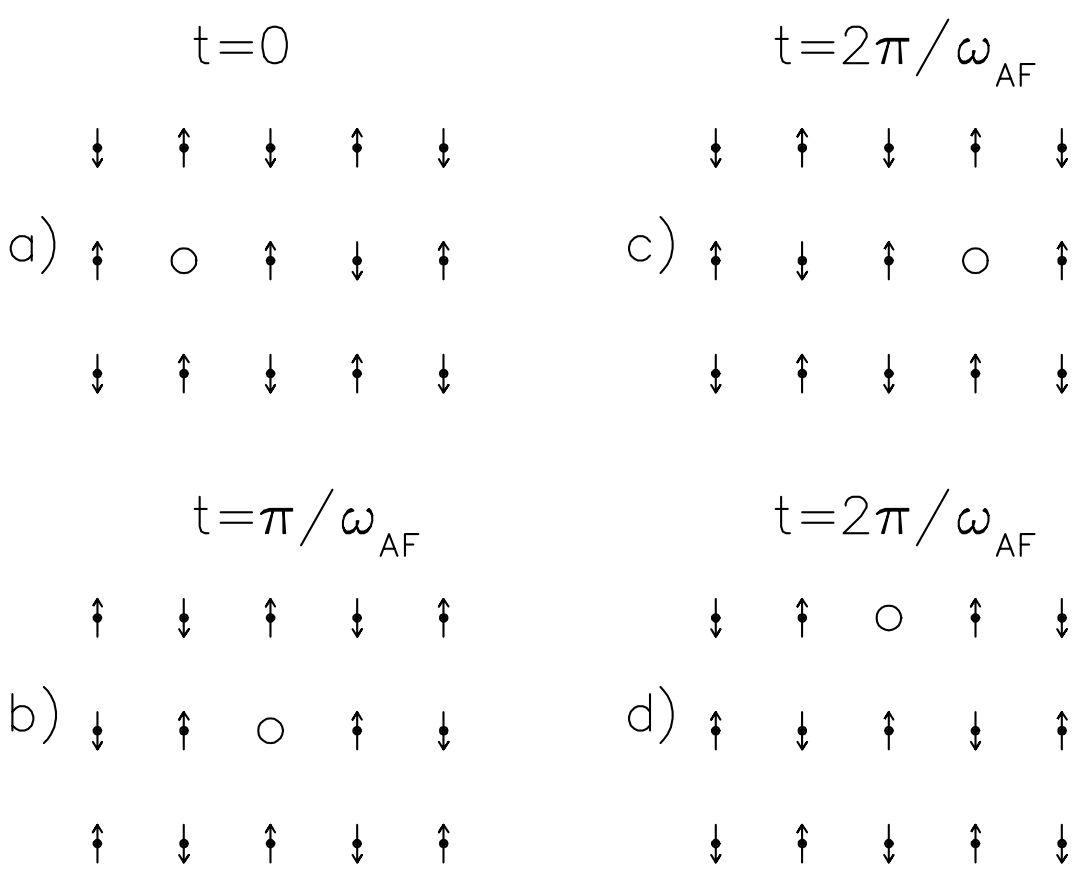

FIG. 9: An illustration of a charge hopping motion in the cuprate resonant with the antiferromagnetic spin fluctuations with the frequency ω_{AF}. (a) is for the $t = 0$ configuration, (b) for the $t = \pi/\omega_{AF}$ after a half period. (c) and (d) show the situation after the full period $t = 2\pi/\omega_{AF}$ for the propagation towards the $(\pi, 0)$ direction and the (π, π) direction, respectively. The charge motion sequenced with AF spin fluctuations helps avoid extra frustration in the charge propagation process.

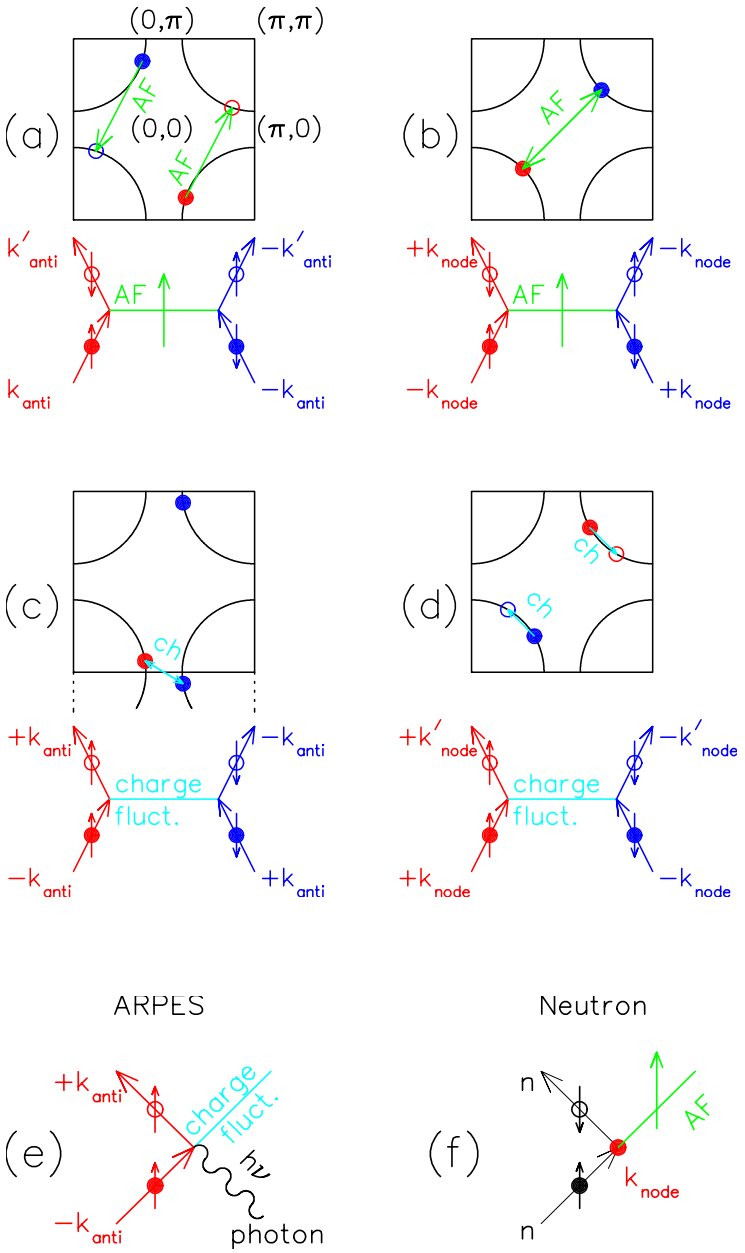

FIG. 10: An illustration of the attractive interaction obtained in the scattering process (a) and (d), and in the binding process (b) and (c) involving the exchange of AF spin fluctuations and charge fluctuations in the cuprates. (e) and (f) show the diagrams for the ARPES coherence peak [23] for antinodal charges (e), and the neutron resonance peak for nodal charges (f), which can be viewed as processes liberating Yukawa-type bonding bosons. These liberation processes occur at a cost of condensation energy, corresponding to the hybrid spin/charge roton energy, with the intensities proportional to the superfluid density n_s/m^*. (a), (c) and (e) show processes for the antinodal charges, while (b), (d) and (f) for nodal charges.